INVESTIGATING INVASION DYNAMICS OF *PSEUDOGYMNOASCUS DESTRUCTANS* IN TEXAS BATS REVEALS DIFFERENTIAL PATTERNS OF PATHOGEN PROGRESSION

By Damian M. Johns

A Thesis

Submitted in Partial Fulfillment

of the Requirements for the Degree of

Master of Science

in Biology

Northern Arizona University

December 2022

Approved:

Jeffrey T. Foster, Ph.D., Chair

Bridget M. Barker, Ph.D.

Joseph R. Hoyt, Ph.D.

ABSTRACT

INVESTIGATING INVASION DYNAMICS OF

PSEUDOGYMNOASCUS DESTRUCTANS IN TEXAS BATS REVEALS

DIFFERENTIAL PATTERNS OF PATHOGEN PROGRESSION

DAMIAN M. JOHNS

As the modern world becomes more connected, the rapid spread of infectious fungal pathogens proves to be one of the leading threats to wildlife health. The fungal disease, white-nose syndrome (WNS), in North American bats is a prominent example of the devastating impact novel pathogens can have on naïve wildlife populations. The virulent disease has caused unprecedented declines in North American bat populations and threatens multiple species with extinction. The causative agent, *Pseudogymnoascus destructans*, is highly adapted to infecting cave-hibernating bats to complete its life cycle, however the extent and severity of WNS threat is highly variable across different bat species and geographic regions. The WNS epizootic presents a unique opportunity to study the disease dynamics and host species impacts of a novel pathogen as it spreads into new regions and populations. The emergence of WNS in the diverse and abundant bat communities of Texas is a significant phase of the pathogen's invasion across the continent and merits examination. Frick et al. (2017) was the first study to examine the spatiotemporal progression of *P. destructans* prevalence and infection intensity during the continental-scale invasion of the pathogen in North America. We aim to build on their foundational study by investigating the prevalence and infection dynamics of *P. destructans* during its invasion and establishment in Texas and how they compare to the progression of the

pathogen in the eastern and midwestern regions of the U.S. Here, we compare the temporal patterns of *P. destructans* progression in *Myotis velifer* and *Perimyotis subflavus* in Texas with the invasion dynamics of the pathogen in the East to better understand the divergent outcomes of host-pathogen interactions.

ACKNOWLEDGEMENTS

First, I would like to thank my advisor, Jeff Foster, for his mentorship and support through this entire experience. Starting graduate school in the middle of a global pandemic came with many challenges and Jeff's dedication to his students and guidance ensured my success and the success of this project. I am also deeply grateful to Diana Northup and Debbie Buecher for graciously adopting me into their field research crew and showing me so many amazing caves and bats. Also, thanks to Judith Ramirez for her mad mist-netting skills.

A special thanks to Katy Parise for taking me under her wing in the lab and teaching me her masterful ways of WNS diagnostics and for always being there to help, even when she didn't have to be.

Thank you to Tina Cheng and Fred Frick for their incredible insight into this system and for their generous assistance with the datasets and statistical analyses. Tina's quantitative ecology chops and R skills made this project possible, and her unwavering encouragement meant so much to me.

Thank you to Bridget Barker and Joe Hoyt for kindly agreeing to be on my committee. Having the support of the leading experts in our field was immensely valuable to this project. I would also like to thank the Foster and Mihaljevic lab groups for their encouragement and for providing helpful feedback on my research. Thank you to all of my lab-mates that contributed to this project by assisting with DNA extractions, qPCR testing, sample organization, making reagents, etc., especially Kelsey Banister and Emma Froehlich.

I would like to sincerely thank the National Science Foundation for funding this research and enabling me to pursue a career in science. I am also extremely thankful to all my collaborators and project partners for their contributions, permits, samples, access to field sites, and hospitality. Shoutout to Brandon Holton, Eathan McIntyre, Erin Lynch, Eric Weaver, and Marikay Ramsey.

Finally, I want to thank my family; thank you to my loving parents for supporting me through all of my endeavors and for facilitating my growth as an inquisitive human, thank you to my brothers and sister for all the laughs and for always believing in me, and thanks to my friends for being a constant source of inspiration and for helping me stay sane. We may be spread out all over the country, but I am forever grateful that we remain close despite the distance. I would not be here if it weren't for the love and support of all the wonderful people in my life.

TABLE OF CONTENTS

LIST OF TABLES

LIST OF FIGURES

CHAPTER TWO

CHAPTER THREE

CHAPTER ONE: A review of white-nose syndrome and the implications of *Pseudogymnoascus destructans* in the West

Wildlife diseases are among the most consequential issues in the fields of conservation and public health today. As the modern world becomes more connected, the rapid spread of infectious fungal pathogens proves to be one of the leading threats to wildlife health (Fisher and Garner, 2020). White-nose syndrome (WNS) is an infectious disease in North American bats caused by the invasive fungus *Pseudogymnoascus destructans*. High-resolution phylogenies of *P. destructans* from whole-genome sequencing indicate the fungal pathogen originated in Europe (Drees et al. 2017). *Pseudogymnoascus destructans* is a psychrophilic (cold-loving) dermatophyte that is highly adapted to and dependent on infecting the epidermal tissue of cave-hibernating bats to complete its life cycle (Wilson et al. 2017, Reynolds & Barton 2014). The parasitic fungus is known to occur on wintering European bats but with no WNS outbreaks or mass mortality events (Puechmaille et al. 2011). However, the disease has caused unprecedented mortality in North America resulting in the collapse of bat populations (Frick et al. 2010, 2017). *Pseudogymnoascus destructans* was first encountered in North America in 2006 in Albany County, New York (Blehert et al. 2009) and continues to spread across the continent with confirmed detections as far as Texas and Washington state (Meierhofer et al. 2021, Lorch et al. 2016). Distinguishing between the positive detection of *P. destructans* and histological confirmation of WNS is important. Bats can test positive for the presence of the pathogen on their body surfaces without exhibiting diagnostic symptoms of the disease.

North American bat species that have been confirmed with WNS are: *Myotis lucifugus, M. sodalis, M. septentrionalis, M. grisescens, M. evotis, M. velifer, M. leibii, M. thysanodes, M.*

volans, M. yumanensis, Perimyotis subflavus, and *Eptesicus fuscus*. Additionally, positive detections of *P. destructans* without diagnostic signs of WNS have been documented in *Corynorhinus rafinesquii, C. townsendii, C. townsendii virginianus, C. townsendii ingens, M. ciliolabrum, Lasiurus borealis, Lasionycteris noctivagans,* and *Tadarida brasiliensis* (US Fish and Wildlife Service, 2022). To date, *P. destructans* has been detected in 39 US states and eight Canadian provinces (US Fish and Wildlife Service 2022), although these numbers refer to published detections below a specific quantitative polymerase chain reaction (qPCR) cycle threshold (C_t) of 37 and low levels (C_t values of 37–40) of the pathogen have been detected in more states. White-nose syndrome has since killed more than six million hibernating bats in North America and threatens multiple species with extinction (Frick et al. 2010, Langwig et al. 2015a, Cheng et al. 2021). The impacts of WNS have been studied extensively in the eastern and midwestern US where most of the mortality has occurred. However, the pathogen continues to spread across the continent into new bat populations and habitats. The implications of the recent arrival of *P. destructans* in the western US, where bat communities are more diverse, are a rapidly growing field of research but are still largely understudied (Hoyt et al. 2021). In addition, the uncertain impacts of climate change compounded with the threat of WNS makes it difficult to predict the future conditions of western bat populations (McClure et al. 2022).

White-nose syndrome manifests as a cutaneous infection that causes significant tissue damage resulting in characteristic lesions on the muzzle and wing membranes of hibernating bats (Meteyer et al. 2009). Tissue damage from the disease can fatally disrupt the physiological homeostasis of infected bats as a result of water and electrolyte imbalances, more frequent arousals from torpor during hibernation, and depletion of crucial fat reserves (Reeder et al. 2012,

Cryan et al. 2013, Warnecke et al. 2013, Verant et al. 2014). The low body temperatures of hibernating bats can prevent the proliferation of most pathogens but suppressed immune function during torpor coupled with the psychrophilic nature of *P. destructans* allows it to overcome these barriers to infection (Field et al. 2015). Bats are also increasingly exposed to an array of human-sourced environmental contaminants and more research is needed to evaluate if exposure to these chemicals could exacerbate WNS infection (Cable et al. 2022).

The extent and severity of WNS threat is highly variable across different bat species and geographic regions (Cheng et al. 2021). The variability in host species declines appears largely dependent on fungal load, with higher fungal loads typically resulting in higher mortality (Langwig et al. 2016, Frick et al. 2017). Higher body fat stores in early winter significantly reduce mortality of *M. lucifugus* by increasing the bats tolerance to the energetic costs associated with WNS (Cheng et al. 2019). The changing physiology of host bat species beginning hibernation drives the seasonal transmission of WNS, with disease prevalence drastically increasing from autumn to late winter and peak *P. destructans* fungal loads in late winter due to the slow growth of the fungus (Langwig et al. 2015a). Direct transmission from bat-to-bat contact is the primary mode of disease spread (Lorch et al. 2011, Hoyt et al. 2018). However, *P. destructans* can persist in the environment for long periods of time without the presence of bats, creating a viable environmental reservoir for the pathogen (Lorch et al. 2013, Hoyt et al. 2015a). Indirect transmission from environmental exposure to *P. destructans* can result in the infection and mortality associated with WNS in naïve bat populations (Hicks et al. 2021). Environmental factors such as temperature and humidity are strong predictors for *P. destructans* growth (Verant et al. 2012, Marroquin et al. 2017). Despite common misconceptions about

hibernacula in the Southwest, many sites are cold and humid enough to support the growth of *P. destructans* (Torres-Cruz et al. 2019). Monitoring bat populations that hibernate in microclimates that are suitable for *P. destructans* growth is critical for early detection of the pathogen. Diagnostic methods of *P. destructans* infection include histopathology, real-time quantitative PCR (qPCR), and ultraviolet fluorescence, with qPCR being the most effective for early detection of the pathogen (McGuire et al. 2016). Many bat species rarely show visual signs of WNS and the use of qPCR testing can provide significantly earlier detection of *P. destructans* than visual surveys alone (Janicki et al. 2015). Quantification of fungal loads via qPCR testing can also reveal the amount of the pathogen that is present and help elucidate the stage and severity of invasion. Investigating infection dynamics during the invasion and establishment of the pathogen allows us to determine the impacts of disease on host populations and identify potential mechanisms of host resistance (Frick et al. 2017).

The destructive mortality events in North America are in stark contrast to the epizoological patterns of *P. destructans* in Europe and Asia, where the fungus is common but seems to remain relatively benign (Hoyt et al. 2015a, 2016, Zukal et al. 2016). The discrepancy of morbidity and mortality between Nearctic and Palearctic bat populations is not well understood but there is evidence for endemicity and tolerance to the fungus in the Palearctic (Zukal et al. 2016). For many places in the world, bat hibernacula (i.e., winter refuges for dormant bats) consist of very large colonies of bats. For example, bats in the eastern and midwestern regions of the US hibernate in densely populated caves with bats numbering in the tens of thousands to hundreds of thousands (Bernard and McCracken 2017). In contrast, typical hibernation behavior of western bats is quite different with bats hibernating individually or in small groups of 2–4 individuals

(Olson and Barclay 2013). Physical contact between western bats during winter is often limited due to small, isolated hibernating groups (Fenton and Barclay 1980). However, there are still many large colonies of hibernating bats in the West that are potentially susceptible to WNS, particularly in the caves of the southwestern region of the US (Hayward 1961). The over-wintering behavior of western bats may reduce their risk of *P. destructans* transmission, but also presents numerous challenges to studying the bats themselves and the spread of the disease in the West (Weller et al. 2018).

Recent WNS epizoological models suggest Texas will play an important role in WNS disease dynamics at the southern leading-edge of infection (Meierhofer et al. 2021). Texas holds both the greatest number of bat species in the U.S. (Schmidly and Bradley 2016) and the largest known bat colonies in the world (Ammerman and Schmidly 2012). *Pseudogymnoascus destructans* was first detected in Texas in multiple hibernating bats in 2017 (Meierhofer et al. 2019), with the first documented case of WNS in a cave myotis (*M. velifer*) in 2020 (Texas Parks and Wildlife Department 2020). Conversely, in eastern bat populations infected with *P. destructans* the onset of WNS occurs relatively quickly, often with high pathogen prevalence and significant declines by the second year after initial invasion (Blehert et al. 2009, Langwig et al. 2015b).

Variability of infection intensity in epidemic and persisting *M. lucifugus* and *P. subflavus* hibernacula suggests that some colonies of these severely impacted species may become resistant or tolerant to the disease (Langwig et al. 2017, Frick et al. 2017). In contrast, infected *M. septentrionalis* colonies exhibit rapid prevalence and fungal load increases until they are extirpated from most sites within three years of *P. destructans* detection, seemingly unable to

control the growth of the fungus (Langwig et al. 2012, Frick et al. 2015, 2017). The precise mechanisms of WNS resistance are unknown. However, a recent study found evidence for genetic adaptation in *M. lucifugus* where surviving bats expressed adaptive shifts in allele frequencies of genes associated with regulating arousal from hibernation, fat breakdown and metabolism, and vocalization/echolocation (Auteri & Knowles 2020). Another potential mechanism of resistance could be the result of changes in the bat skin microbiome after infection, allowing for greater inhibition of *P. destructans* growth (Hoyt et al. 2015b). A study investigating skin microbial composition in three North American bat species (*M. lucifugus*, *Eptesicus fuscus*, and *Perimyotis subflavus*) found that WNS significantly restructures the skin microbiome of *M. lucifugus*, lowering the abundance of key bacterial families that could be involved in pathogen defense. Interestingly, the skin bacterial diversity of *E. fuscus* and *P. subflavus* were unaffected despite all three species experiencing drastic declines in some populations (Ange-Stark et al. 2019). Microbial skin assemblages, particularly yeast diversity and abundance, are strongly associated with WNS resistance in eastern bats (Vanderwolf et al. 2021a). Recent modeling based on bat skin fungal assemblages predicted WNS susceptibility in 13 western bat species and found only one species, *Myotis velifer*, predicted to be WNS resistant (Vanderwolf et al. 2021b). However, the emergence of the disease in Texas *M. velifer* (Texas Parks and Wildlife Department 2020) indicates the species is still susceptible to WNS.

To date, researchers have been unable to identify effective treatments for WNS. Recent advances in potential mitigation strategies for reducing WNS impacts include the treatment of bats with a probiotic bacterium (*Pseudomonas fluorescens*), however these treatments may only offer temporary protection from the pathogen (Cheng et al. 2017, Hoyt et al. 2019) and the

applicability in the West is unknown. Additionally, a study on the efficacy of four different WNS vaccine treatments in captive *M. lucifugus* showed potential for the use of virally vectored vaccines in inducing an immune response against *P. destructans* (Rocke et al. 2019). However, the efficacy in other susceptible bat species is unknown and the implementation of a vaccine into wild bat populations is complicated. The use of population viability models could help facilitate the recovery of WNS-affected populations by determining the trajectory of those treated with different WNS mitigation methods (Fletcher et al. 2020). The ability of *P. destructans* to persist in the environment for long periods of time after bats are extirpated may prevent the recolonization of hibernation sites, further complicating the issue and increasing the extinction risk of affected bats (Hoyt et al. 2015a).

Phenotypic variation of *P. destructans* across the geographic invasion gradient from eastern North America suggests the ability of the pathogen to adapt and acclimatize to varying environmental conditions (Forsythe et al. 2018). This presents additional uncertainty for the future of western bat habitats as the fungus could potentially evolve phenotypic adaptations to the more arid environments of the West. The devastating impacts of WNS have created an urgent need for further study into the disease dynamics and host-pathogen interactions of novel species. Ultimately, public outreach and education will play a key role in the conservation of bats and the management of caves across US public lands (Shapiro et al. 2021).

CHAPTER TWO: Investigating invasion dynamics of *Pseudogymnoascus destructans* in Texas bats reveals differential patterns of pathogen progression

INTRODUCTION

White-nose syndrome (WNS) is a virulent disease in North American bats caused by the invasive fungus, *Pseudogymnoascus destructans*. The fungal pathogen, *P. destructans*, is a psychrophilic (cold-loving) dermatophyte that is highly adapted to and dependent on infecting the epidermal tissue of cave-hibernating bats to complete its life cycle (Wilson et al. 2017, Reynolds & Barton 2014). The disease has caused unprecedented mortality in North America resulting in the collapse of bat populations (Frick et al. 2010, 2017). *Pseudogymnoascus destructans* was first encountered in North America in 2006 (Blehert et al. 2009) and continues to spread across the continent with confirmed detections as far as Texas and Washington state (Meierhofer et al. 2021, Lorch et al. 2016). Distinguishing between the positive detection of the pathogen and histological confirmation of the disease is important. Bats can test positive for the presence of *P. destructans* on their body surfaces without exhibiting diagnostic symptoms of WNS.

To date, *P. destructans* has been detected in 39 U.S. states and eight Canadian provinces (US Fish and Wildlife Service 2022). Although, these numbers refer to published detections below a specific quantitative polymerase chain reaction (qPCR) cycle threshold (C_t) of 37, and low-level positives (C_t values of 37–40) of the pathogen have been detected in more states. White-nose syndrome has been confirmed in 12 North American bat species and another eight species have tested positive for *P. destructans* (US Fish and Wildlife Service 2022). The disease has since killed more than six million bats in North America, and threatens multiple species with extinction (Frick et al. 2010, Langwig et al. 2015a, Cheng et al. 2021). Many bat species rarely show visual signs of WNS, and the use of qPCR testing can provide significantly earlier

detection of *P. destructans* than visual surveys alone (Janicki et al. 2015). Quantification of fungal loads with qPCR testing can also reveal the amount of the pathogen that is present and help elucidate the stage and severity of infection. Investigating infection dynamics during the invasion and establishment of the pathogen allows us to better understand the variable impacts of disease on host populations and identify potential mechanisms of host resistance (Frick et al. 2017).

The variability in host species impacts is strongly associated with temperature and humidity (Verant et al. 2012, Marroquin et al. 2017). In addition, WNS mortality is largely dependent on fungal load, with higher fungal loads typically resulting in higher mortality (Langwig et al. 2016, Frick et al. 2017). The disease disrupts the physiological homeostasis of infected bats by causing epidermal tissue damage resulting in water and electrolyte imbalances, more frequent arousals from torpor during hibernation, and depletion of crucial fat reserves (Reeder et al. 2012, Cryan et al. 2013, Warnecke et al. 2013, Verant et al. 2014). The changing physiology of host bat species beginning hibernation drives the seasonal transmission of WNS, with disease prevalence drastically increasing from autumn to late winter and peak *P. destructans* fungal loads in late winter due to the slow growth of the fungus (Langwig et al. 2015a). The low body temperatures of hibernating bats can prevent the proliferation of most pathogens but suppressed immune function during torpor coupled with the psychrophilic nature of *P. destructans* allows the fungus to overcome these barriers to infection (Field et al. 2015).

The extent and severity of WNS threat is highly variable across different bat species and geographic regions (Cheng et al. 2021). Recent WNS epizoological models suggest Texas will

play an important role in WNS disease dynamics at the southern leading-edge of infection (Meierhofer et al. 2021). Texas holds both the greatest number of bat species in the U.S. (Schmidly and Bradley 2016) and the largest known bat colonies in the world (Ammerman and Schmidly 2012). Interestingly, Texas is where we first started seeing a change in the typical disease dynamics of WNS. *Pseudogymnoascus destructans* was first detected in Texas in multiple hibernating bats in 2017 (Meierhofer et al. 2019), with the first documented case of WNS in a cave myotis (*Myotis velifer*) in 2020 (Texas Parks and Wildlife Department 2020). Conversely, in eastern bat populations infected with *P. destructans* the onset of WNS occurs relatively quickly, often with high pathogen prevalence and significant declines by the second year after initial invasion (Langwig et al. 2015b).

Variability of infection intensity in epidemic and persisting *M. lucifugus* and *P. subflavus* hibernacula suggests that some colonies of these severely impacted species may have become resistant or tolerant to the disease (Langwig et al. 2017, Frick et al. 2017). In contrast, infected *M. septentrionalis* colonies exhibit rapid prevalence and fungal load increases until they are extirpated from most sites within three years of *P. destructans* detection, seemingly unable to control the growth of the fungus (Langwig et al. 2012, Frick et al. 2015, 2017). The precise mechanisms of host species persistence are unknown. However, evidence for genetic adaptation was found in *M. lucifugus* where surviving bats expressed adaptive shifts in allele frequencies of genes associated with regulating arousal from hibernation, fat breakdown and metabolism, and vocalization/echolocation (Auteri & Knowles 2020). Another potential mechanism of resistance could be the result of changes in the bat skin microbiome after infection, allowing for greater inhibition of *P. destructans* growth (Hoyt et al. 2015b). A study investigating skin microbial

composition in three North American bat species (*M. lucifugus*, *Eptesicus fuscus*, and *P. subflavus*) found that WNS significantly restructures the skin microbiome of *M. lucifugus*, lowering the abundance of key bacterial families that could be involved in pathogen defense. Interestingly, the skin bacterial diversity of *E. fuscus* and *P. subflavus* were unaffected despite all three species experiencing drastic declines in some populations (Ange-Stark et al. 2019).

Phenotypic variation of *P. destructans* across the geographic invasion gradient from eastern North America suggests the ability of the pathogen to adapt and acclimatize to varying environmental conditions (Forsythe et al. 2018). This presents uncertainty for the future of Western bat habitats as the fungus could potentially evolve phenotypic adaptations to the more arid environments of the West. The WNS epizootic presents a rare opportunity to study the disease dynamics of a novel pathogen as it spreads into new regions and host populations. The emergence of WNS in the abundant and diverse bat communities of Texas is a significant phase of the pathogen's invasion across the continent.

Frick et al. (2017) was the first study to examine the spatiotemporal progression of *P. destructans* prevalence and infection intensity during the continental-scale invasion of the pathogen in North America. We aim to build on their foundational study by investigating the prevalence and infection dynamics of *P. destructans* during its invasion and establishment in Texas and how they compare to the progression of the pathogen in the eastern and midwestern regions of the US. Here, we compare the temporal patterns of *P. destructans* progression in *Myotis velifer* and *Perimyotis subflavus* in Texas with the invasion dynamics of the pathogen in the East to better understand the divergent outcomes of host-pathogen interactions.

METHODS

Overview

In this study we applied the statistical methodology used in Frick et al. (2017) to conduct a comparative analysis of *P. destructans* invasion dynamics between Texas and the eastern and midwestern regions of the US (Here, we'll refer to the midwestern and eastern regions of the US collectively as the "East"). We investigated pathogen invasion dynamics by evaluating the temporal progression *P. destructans* prevalence between two bat species that occur in Texas (*Myotis velifer* (MYVE) and *Perimyotis subflavus* (PESU)) and five eastern bat species (*M. septentrionalis* (MYSE), *M. lucifugus* (MYLU), *P. subflavus* (PESU), *M. sodalis* (MYSO), *Eptesicus fuscus* (EPFU). Model predictions were produced in R using the same dataset used in Frick et al. (2017) with *P. destructans* surveillance data added from *M. velifer* and *P. subflavus* in Texas.

Data collection

The field sampling for this study consisted of two major *P. destructans* surveillance efforts in the US, culminating in two distinct datasets. First, internal hibernacula surveys were conducted during winters at 167 sites across the eastern and midwestern regions of the US between 2009 and 2015 to create the "eastern" dataset (Frick et al. 2017). Second, biologists sampled hibernating bats for *P. destructans* at 151 sites across Texas during winters from 2014 to 2022 to produce the Texas dataset. Bat swab samples were collected using a standardized swabbing protocol (Frick et al. 2017). Epidermal swab sampling involved dipping a sterile polyester swab in sterile molecular grade water and rubbing the swab across the bat's muzzle and a forearm 5 times (Langwig et al. 2015a). Swab samples were stored in 2 mL sterile cryovials in RNAlater

from the field to the lab and stored at -20°C until they were processed. We processed and analyzed the samples in the Pathogen and Microbiome Institute BSL2 laboratory at Northern Arizona University. DNA from bat swab samples were extracted using DNeasy Blood and Tissue extraction kits (Qiagen, Valencia, CA) with a modification for fungal extractions to include lyticase in addition to proteinase K and ATL buffer during the lysis step (Shuey et al. 2014). We tested for the presence and quantity of *P. destructans* DNA following the Muller et al. (2013) protocol, using a real-time qPCR assay. Each sample was tested in duplicate and considered positive for *P. destructans* if at least one qPCR run amplified below a cycle threshold (C_t) of 40 (Frick et al. 2017).

Statistical analyses

P. destructans in Texas: *Myotis velifer* analysis

We used the same generalized linear mixed effects model used in Frick et al. (2017) to model the temporal progression of *P. destructans* presence/absence in *M. velifer*, where prevalence is the response variable and each bat swab sample is a data point with site as a random effect:

$$pd\ species + r1ysi + daysHs + r1ysi{:}species + daysHs{:}species + daysHs{:}r1ysi + (1|site),family = binomial$$

Here, *ysi* is years since *P. destructans* detection at a site and is determined by the winter year of sampling minus the year of *P. destructans* arrival to a site (transformed into *r*1*ysi*):

$$r1ysi = 1 - (1/(ysi+1))$$

The predictor variable *daysH* is days in hibernation (the number of days a species has been in hibernation at the time of *P. destructans* sampling) and is measured as the difference between the sampling day and the first day of hibernation. *daysHs* is scaled *daysH* and is calculated as:

$$daysHs=(daysH-mean(daysH))/sd(daysH)$$

We ran the full model using the same dataset used in Frick et al. (2017) but added *P. destructans* surveillance data for *M. velifer* from Texas. We conducted pairwise comparisons of individual species against *M. velifer* to provide a deeper look at predicted lines with 95% confidence intervals. Examining overlap in 95% confidence intervals of predicted lines allows us to better understand whether differences in annual trends are significant (i.e., a lack of overlap in 95% confidence intervals indicates that differences are statistically significant). We then examine pairwise comparisons of early and late winter *P. destructans* prevalence dynamics of *M. velifer* versus 5 other bat species included in Frick et al. (2017) by analyzing predicted lines with 95% confidence intervals. Here, "early winter" is the first day of hibernation and "late winter" is 142 days into hibernation. We fit the mixed effects models using R version 4.0.2 with package glmmTMB.

P. destructans in Texas: *Perimyotis subflavus* analysis

We compared *P. destructans* prevalence by years since detection and days in hibernation for *P. subflavus* in Texas versus the rest of the species' range in the East. We used generalized linear mixed effects models (R package glmmTMB) fitting *P. destructans* presence/absence data to a binomial distribution and included years since *P. destructans* detection, days in hibernation, and site as a random effect. We asked whether *P. subflavus* in Texas exhibited different trends in *P. destructans* prevalence over time by including *Texas* as a covariate, with *P. subflavus* existing in the rest of the species' range noted as *other*. We also tested models that included latitude and

both latitude and longitude as covariates to identify the best-fit model including all potential spatial delineations. We allowed for a non-linear relationship between *P. destructans* prevalence and years since detection by transforming years since *P. destructans* detection using a non-linear transformation, as done in Frick et al. (2017). We compared models based on Akaike's Information Criterion (AIC: Anderson and Burnham 2002) to determine the best-fit transformation of all predictor variables and the two-way interactions between them. We chose the best-supported model as the model with the lowest AIC value and if it had at least two AIC points less than the next model. The *Texas* covariate was a significant predictor (Table S2, P = 0.002) for *P. destructans* prevalence and was included in the final model:

$$pd\ species + r1ysi + daysHs + daysHs{:}r1ysi + texas + texas{:}daysHs + texas{:}r1ysi + (1|site),\ family = binomial$$

RESULTS

P. destructans in Texas: Myotis velifer analysis

For the *M. velifer* analysis, 3,014 samples from *M. velifer* were collected at 24 sites across Texas and 4,367 samples were collected from 5 species at 132 sites across the eastern US (Table 1). In the first year of detection (year = 0) across all sites, the proportion of bats infected with *P. destructans* was very low for *M. velifer* (Figure 1.1) Prevalence increased at relatively low rates in the 5 eastern species, but all rose above 50% by the end of hibernation (Figure 1.1). Beginning in the first year following *P. destructans* detection, prevalence in *M. velifer* increased at significantly lower rates compared to *M. septentrionalis*, *M. lucifugus*, *P. subflavus*, and *M. sodalis* but at rates relatively similar to *E. fuscus*. As the pathogen becomes established in subsequent years, *P. destructans* prevalence starts high (above 50%) and saturates close to 100%

in early winter for *M. septentrionalis*, *M. lucifugus*, *P. subflavus*, and *M. sodalis*. However, for *M. velifer* and *E. fuscus*, prevalence continues to start low (below 50%) in early winter and increase through hibernation to levels near 100% by late winter (Figure 1.1).

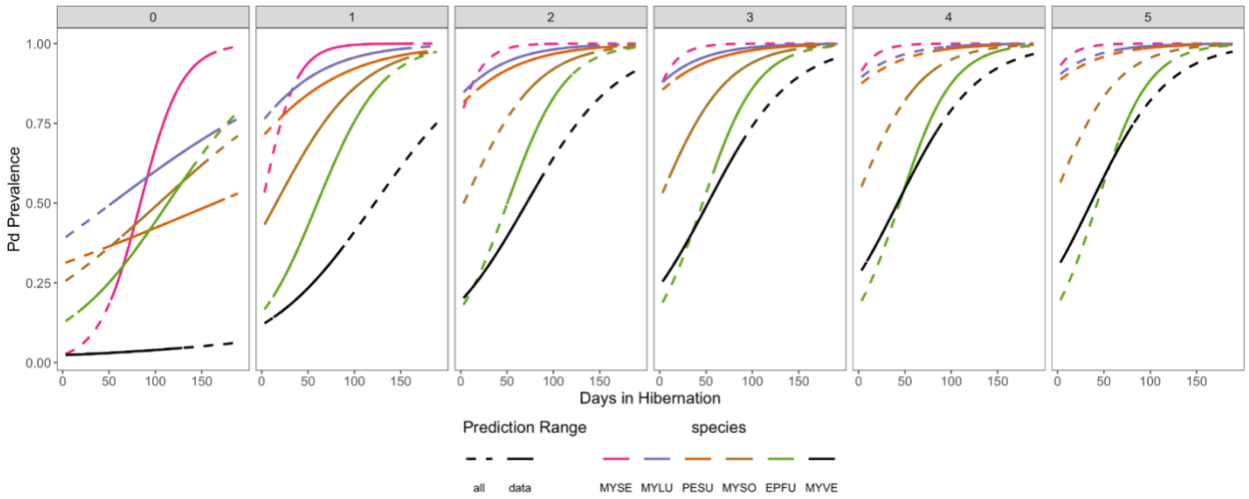

Figure 1.1. *Pseudogymnoascus destructans* prevalence by days in hibernation and years since detection comparing all species to each other. Model predictions (lines) are shown for six species of hibernating bats (colors) with progression of Pd prevalence by days in hibernation (x-axis) and years since Pd detection (horizontal panels). Predictions overlapping where raw data exist are indicated by solid lines and extended predictions beyond the range of the data are indicated by dashed lines.

The progression of *P. destructans* infection was variable between species both during hibernation each winter and across years since initial invasion (Figure 1.1). However, all species in the study except *M. velifer* showed an increase in prevalence above 90% by late winter in the first year after initial detection (year = 1, Figure 1.1). Infection intensity was most severe in *M. septentrionalis*, *M. lucifugus*, and *P. subflavus*, with prevalence in *M. septentrionalis* surging above 90% in the year of initial detection (Figures 1.1, 1.2). The increase of *P. destructans* prevalence in *M. velifer* was significantly different from *M. septentrionalis*, *M. lucifugus*, and *P. subflavus*, with prevalence increasing at lower rates both within each winter and year-to-year in comparison to those eastern species (Figure 1.2). The prevalence of *P. destructans* between *M. velifer* and *M. sodalis* were significantly different during the first two years of invasion with the

same trend of lower rates of increase in *M. velifer*, but their prevalence rates begin to converge in the second year following initial invasion (year = 2, Figure 1.2).

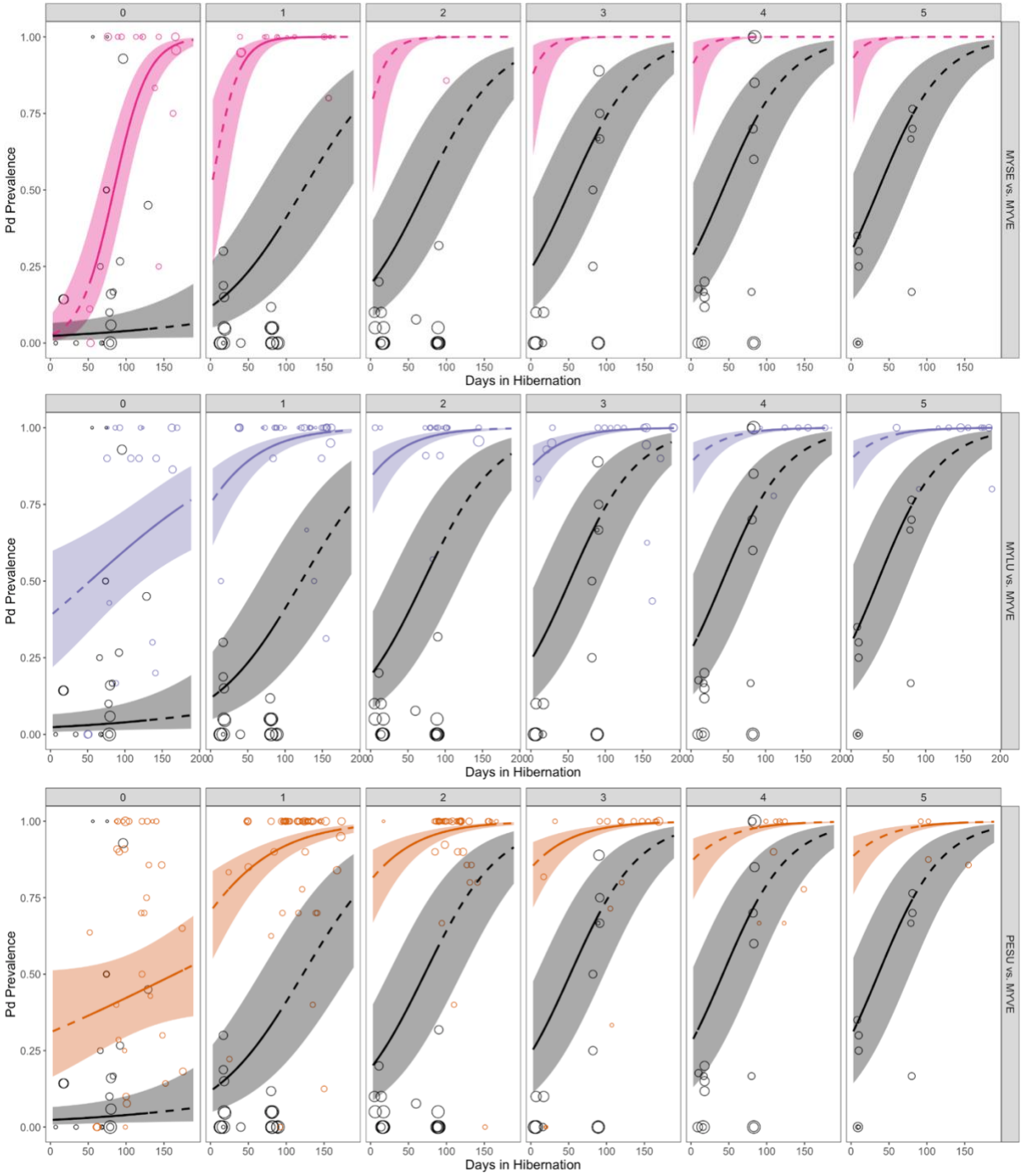

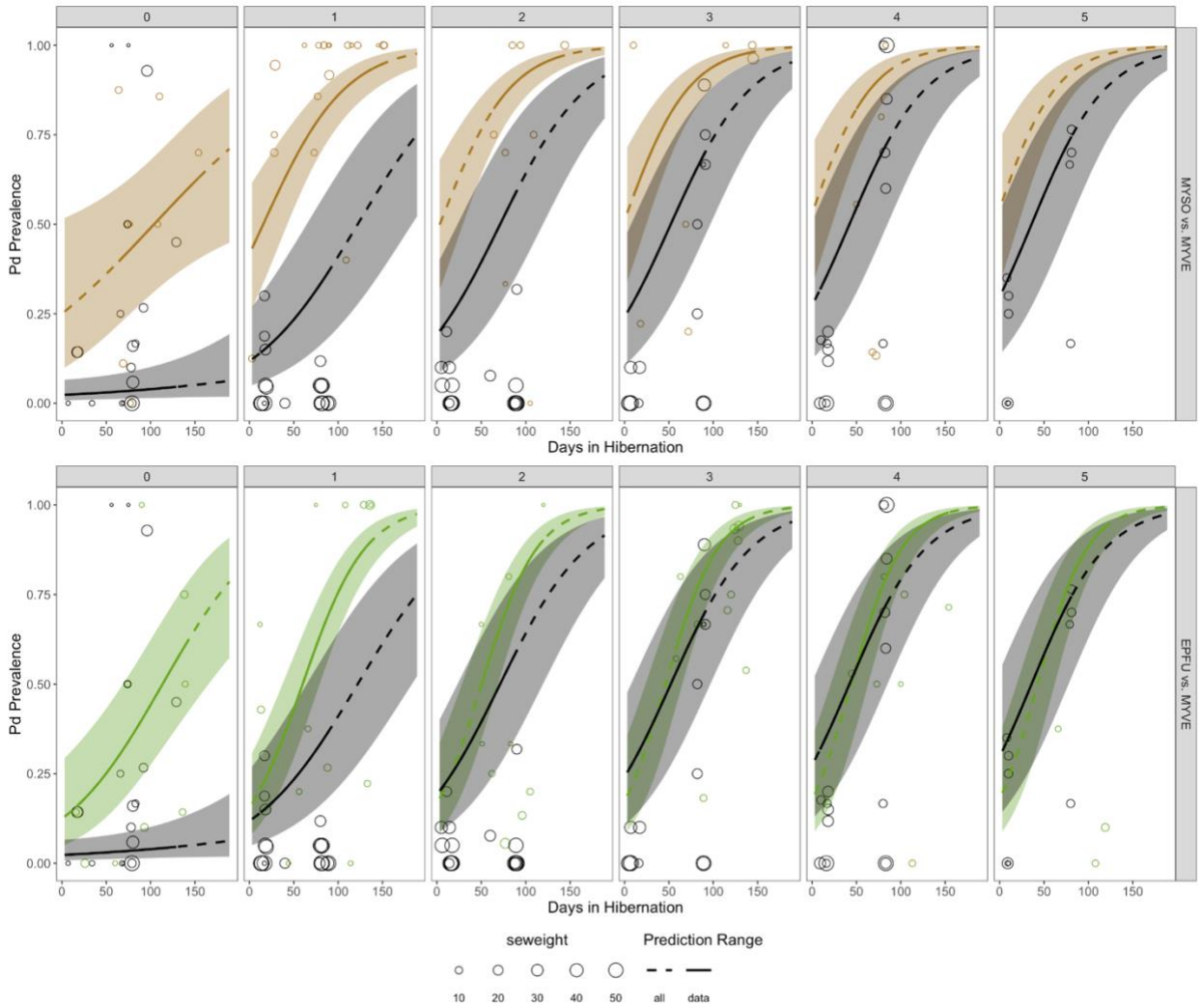

Figure 1.2. Progression of *Pseudogymnoascus destructans* prevalence by days in hibernation and years since Pd detection are compared between Myotis velifer and other bat species. Model predictions (lines) with 95% confidence intervals (shaded areas) are shown for Pd prevalence by days in hibernation (x-axis) and years since Pd detection (years 0–5, horizontal panels) comparing *Myotis velifer* (MYVE, black lines and points) with the following species (vertical panels): *M. septentrionalis* (MYSE), *M. lucifugus* (MYLU), *Perimyotis subflavus* (PESU), *M. sodalis* (MYSO), and *Eptesicus fuscus* (EPFU). Model predictions overlapping raw data (points) are indicated as solid lines with thick shaded 95% confidence intervals and extended model predictions extending beyond the sampled data range are indicated as dotted lines with less shaded confidence intervals. Raw data points are weighted by the inverse of the binomial error for each data point.

Annual dynamics in early winter indicate *M. velifer* has much lower rates of *P. destructans* prevalence increase from year-to-year in comparison to *M. septentrionalis*, *M. lucifugus*, *P. subflavus*, and *M. sodalis* and at rates closer to *E. fuscus* (Figure 1.3). Annual trends in late winter are less different but still show the same pattern of *M. velifer* exhibiting lower rates of prevalence increase each year than all the other species, including *E. fuscus* (Fig. 1.3). Annual

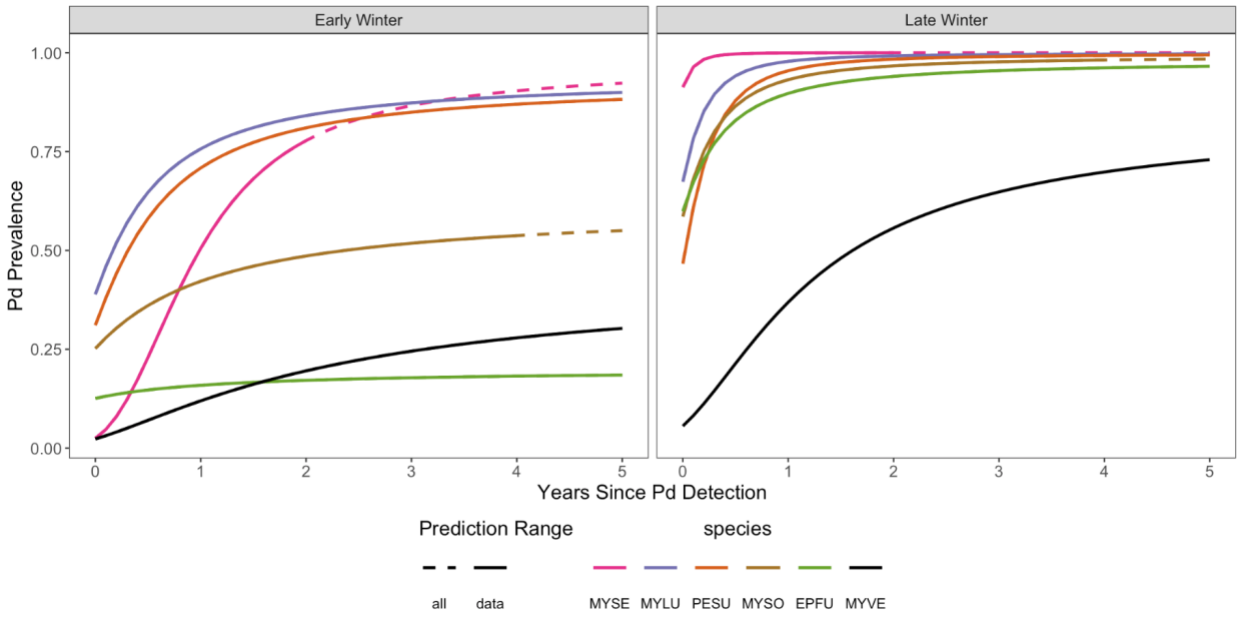

Figure 1.3. *Pseudogymnoascus destructans* prevalence by years since Pd detection comparing all species to each other in early winter (day one of hibernation, left panel) and late winter (day 142 of hibernation, right panel). For *M. velifer*, we predicted late winter Pd prevalence by years since Pd detection on day 89 of hibernation, which is roughly the anticipated end of hibernation for *M. velifer* in Texas (black line). Model predictions (lines) are shown for six species of hibernating bats (colors) with progression of Pd prevalence by years since Pd detection. Predictions overlapping where raw data exist are indicated by solid lines and extended predictions beyond the range of the data are indicated by dashed lines.

prevalence dynamics in *M. velifer* differed significantly from *M. septentrionalis*, *M. lucifugus* and *P. subflavus*, with lower rates of prevalence increase in both early and late winter (Figure 1.4). This trend is most apparent in early winter when *P. destructans* prevalence stays at low levels (below 50%) in *M. velifer* with ongoing years since detection, while prevalence in *M. septentrionalis*, *M. lucifugus* and *P. subflavus* is greater than 50% in early winter after the first year of invasion (Figure 1.4).

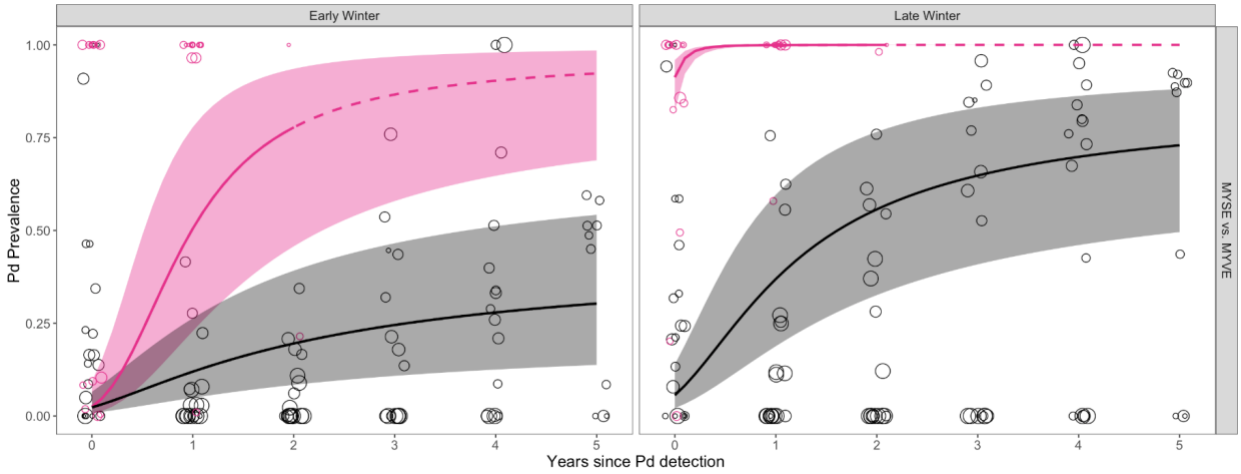
Early Winter
Late Winter
MYSE vs. MYVE
Pd Prevalence
1.00
0.75
0.50
0.25
0.00
0
1
2
3
4
5
Years since Pd detection

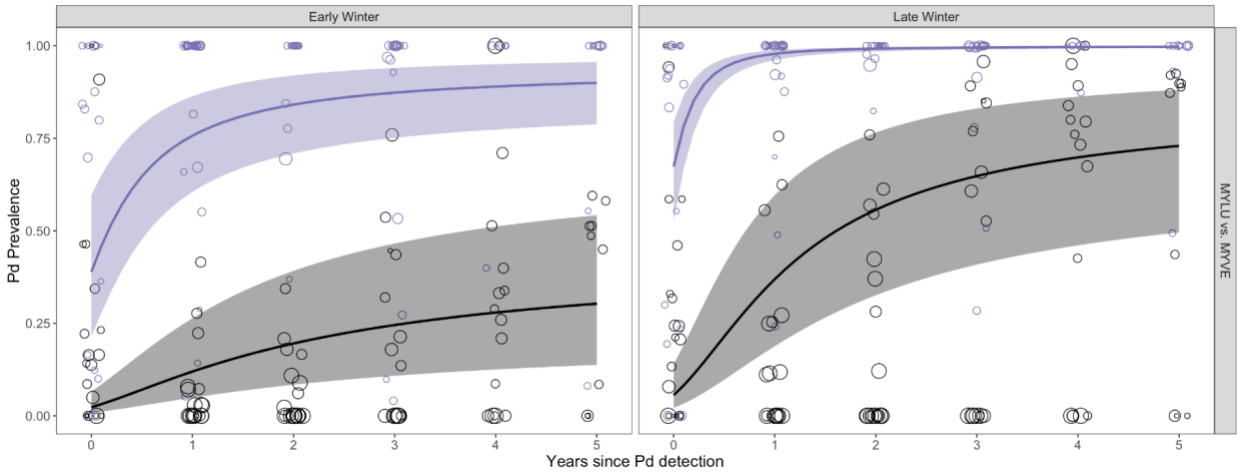
Early Winter
Late Winter
MYLU vs. MYVE
Pd Prevalence
1.00
0.75
0.50
0.25
0.00
0
1
2
3
4
5
Years since Pd detection

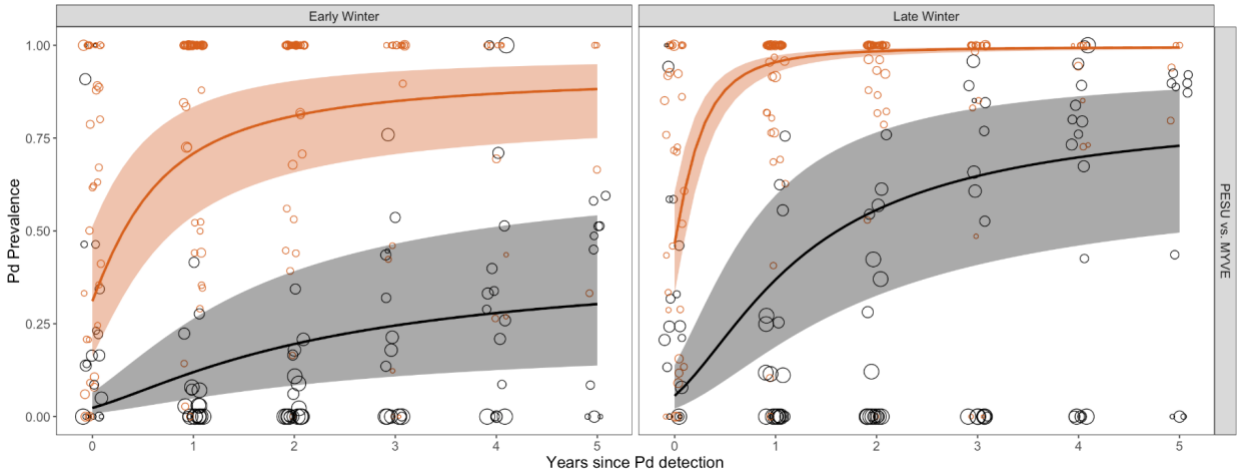
Early Winter
Late Winter
PESU vs. MYVE
Pd Prevalence
1.00
0.75
0.50
0.25
0.00
0
1
2
3
4
5
Years since Pd detection

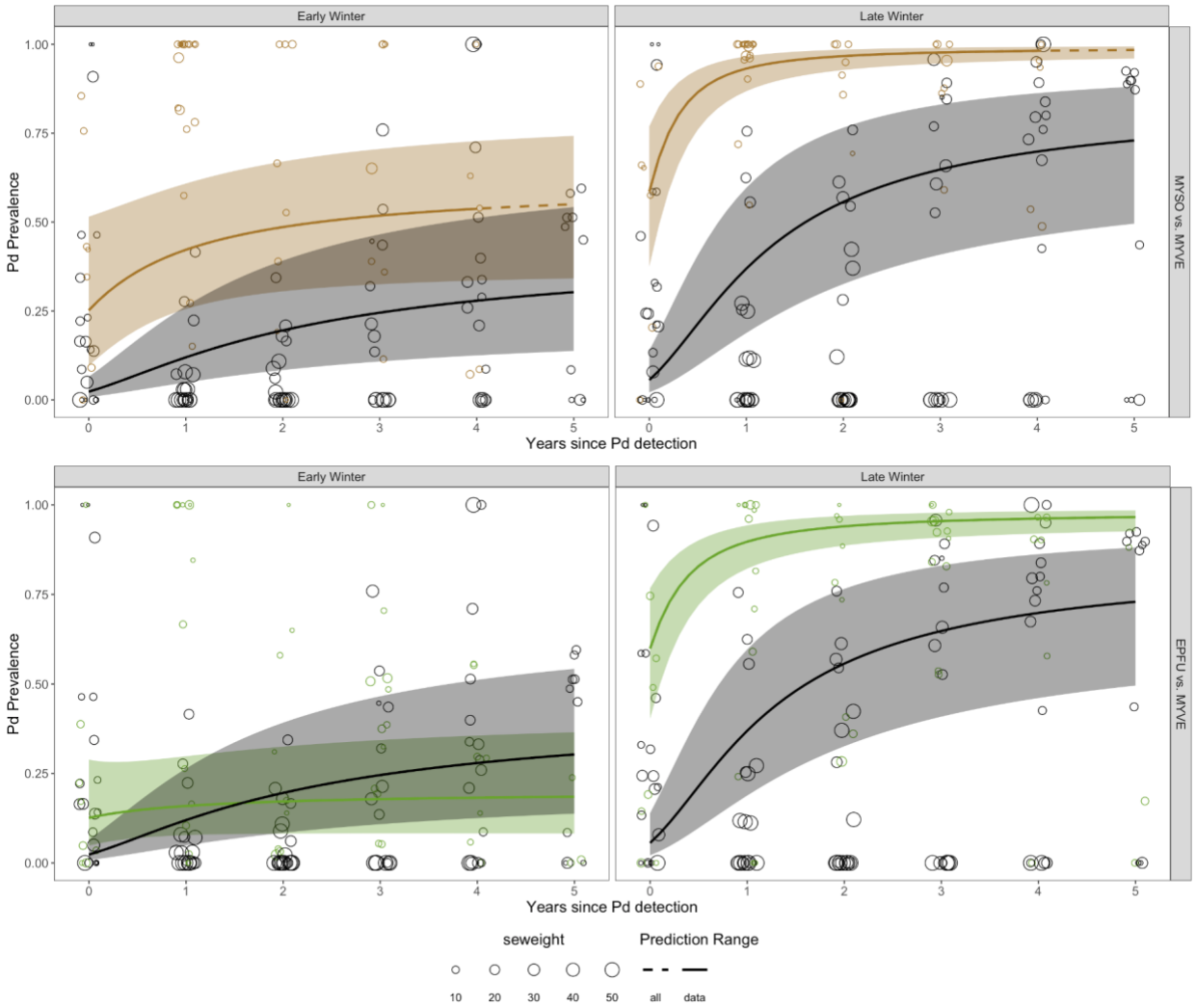

Figure 1.4. Progression of *Pseudogymnoascus destructans* prevalence in early and late winter by years since detection compared between *Myotis velifer* and other bat species. Comparison of annual Pd progression between *M. velifer* and other bat species in early winter (first day of hibernation) and late winter (day 142 of hibernation). Model predictions (lines) with 95% confidence intervals (shaded areas) are shown for Pd prevalence by years since Pd detection comparing *M. velifer* (MYVE, black lines and points) with the following species (vertical panels): *M. septentrionalis* (MYSE), *M. lucifugus* (MYLU), *Perimyotis subflavus* (PESU), *M. sodalis* (MYSO), and *Eptesicus fuscus* (EPFU). For *M. velifer*, we predicted late winter Pd prevalence by years since Pd detection on day 89 of hibernation, which is roughly the estimated end of hibernation for *M. velifer* (black line in late winter panel). Model predictions overlapping raw data (points) are indicated as solid lines with thick shaded 95% confidence intervals and extended model predictions extending beyond the sampled data range are indicated as dotted lines with less shaded confidence intervals. Raw data points are weighted by the inverse of the binomial error for each data point.

P. destructans in Texas: Perimyotis subflavus analysis

For the *P. subflavus* analysis, 1,160 samples were collected at 17 sites across Texas and 1,550 samples were collected at 89 sites across the eastern US (Table 2). Comparing pathogen invasion dynamics between *P. subflavus* colonies in Texas versus the rest of the species' range in the East

reveals a pattern of reduced infection intensity in Texas. Examining *P. destructans* prevalence by days in hibernation indicates a significant difference in the within-winter dynamics between the two *P. subflavus* metapopulations. In the first year of *P. destructans* detection, *P. subflavus* in Texas exhibit lower rates of prevalence increase than eastern populations but culminate into similar levels by the end of hibernation (Figure 1.5). However, by the following winter there is a significant difference in *P. destructans* prevalence at the beginning of hibernation, with Texas *P. subflavus* starting at levels similar to the initial year of detection and eastern populations starting close to 90% prevalence (Figure 1.5). This trend continues every year during pathogen invasion with Texas *P. subflavus* starting at low prevalence levels in early winter and eastern populations starting above 90% each year, eventually saturating near 100% prevalence (Figure 1.5).

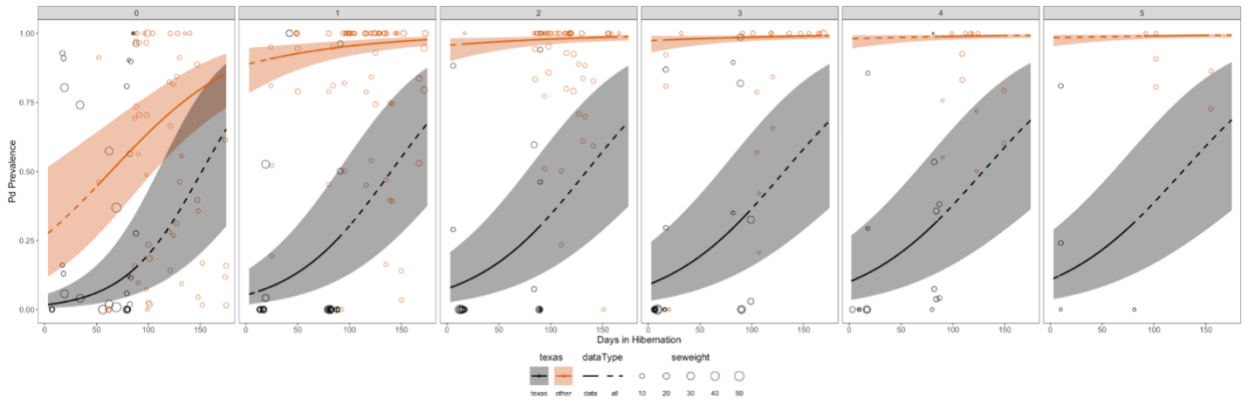

Figure 1.5. *Pseudogymnoascus destructans* prevalence by days in hibernation and years since Pd detection in *Perimyotis subflavus*. Fitted lines with 95% confidence intervals (shaded areas) for Pd prevalence from the best-supported model are shown for *P. subflavus* from Texas (black lines and points) versus the rest of the species' range (other; orange lines and points). Raw Pd prevalence is plotted by site with size of point representing the inverse of the binomial error.

The annual progression of *P. destructans* prevalence in Texas *P. subflavus* colonies was significantly slower than colonies in the East (Figure 1.6). Infection prevalence increased rapidly in the majority of eastern *P. subflavus* colonies, reaching 100% by late winter in year 2 after initial invasion (Figure 1.6). Conversely, the majority of *P. subflavus* colonies in Texas never

reach 100% infection prevalence after 5 years of pathogen invasion (Figure 1.6). Eastern colonies exhibit higher prevalence by the end of each subsequent winter until reaching 100%. However, prevalence in Texas *P. subflavus* colonies appears to stagnate at similar levels by the end of each winter, usually peaking between 50% and 75% (Figure 1.6).

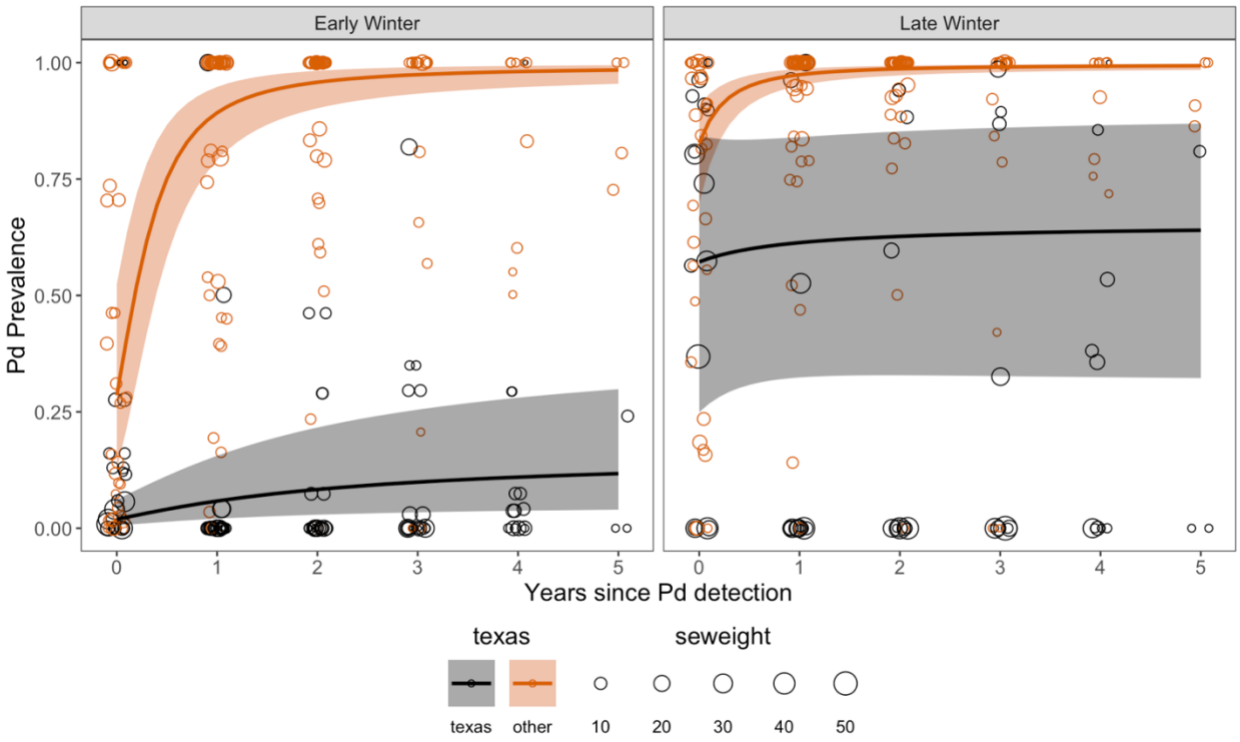

Figure 1.6. Progression of *Pseudogymnoascus destructans* prevalence by years since Pd detection are compared between *Perimyotis subflavus* in Texas versus the rest of the species' range. Comparison of annual Pd progression between *P. subflavus* is shown for early winter (left) and late winter (right). Model predictions (lines) with 95% confidence intervals (shaded areas) are shown for Pd prevalence by years since Pd detection comparing *P. subflavus* in Texas (black lines and points) with the rest of the species' range (orange lines and points). Model predictions overlapping raw data (points) are indicated as solid lines with thick shaded 95% confidence intervals and model predictions extending beyond the sampled data range are indicated as dotted lines with less shaded confidence intervals. Raw data points are weighted by the inverse of the binomial error for each data point.

DISCUSSION

Our results illustrate a clear pattern of slowed *P. destructans* progression during invasion and establishment in Texas and a delayed onset of WNS when compared to disease dynamics in the East. We found evidence for a reduction in the rate of prevalence increase in both the within-

winter and year-to-year pathogen dynamics of both Texas bat species in the study, *M. velifer* and *P. subflavus* (Figures 1.1, 1.5). Interestingly, the infection dynamics of *M. velifer* resembled those of *E. fuscus* after the first year of invasion (Figure 1.2), a species shown to be less susceptible to WNS compared to other bat species (Langwig et al. 2012). By making an intraspecific comparison of pathogen prevalence in *P. subflavus* occurring in Texas versus the rest of the species' range in the East, we were able to determine that the divergent *P. destructans* dynamics are not simply an interspecific difference (Figure 1.5). The delay of WNS progression in Texas after the arrival of *P. destructans* in 2017 suggests the ecology and effects of the pathogen may be different from the disease dynamics that have been documented in the East, at least in more northern latitudes.

Various attributes of both the bats and their hibernacula are likely contributing to the differences in WNS disease dynamics between Texas and the eastern US. Shortened hibernation duration of *M. velifer* could be slowing *P. destructans* progression in Texas hibernacula, making it harder for the pathogen to stabilize and become established. It is possible that *M. velifer* are more active during the winter and reduce the ability of the fungus to establish itself in Texas colonies. The slower *P. destructan*s progression in Texas hibernacula could be due to a difference in the bat-to-environment transmission and environment-to-bat transmission. Texas *M. velifer* and *P. subflavus* colonies appear to have significantly lower rates of pathogen transmission in early hibernation compared to colonies in the East (Figure 1.6). Low early-winter prevalence in *M. velifer* and Texas *P. subflavus* suggests there is less of the fungus present on the bats entering hibernation or in the substrate of their roost environment.

It appears that as the pathogen becomes established, the environmental reservoir for *P. destructans* in Texas hibernacula does not continually build up to higher prevalence and fungal loads in the same way as eastern hibernacula. Instead, pathogen prevalence significantly drops off after winter each year, resetting to similar levels in the beginning of the previous winter. Further study into the temporal patterns of prevalence and fungal loads in Texas hibernacula environmental samples is needed to make this determination. The different climatic conditions in Texas could explain why *P. destructans* does not appear to proliferate and stabilize as well in Texas hibernacula compared to the East. However, the internal climates of certain Texas karst systems do show seasonally varying patterns of suitability for *P. destructans* growth and are likely able to sustain the fungus enough to cause disease and resulting declines in Texas bats (Wolf et al. 2022). Additionally, in many Texas and Oklahoma hibernacula, *M. velifer* form large, dense clusters in microclimates within the optimal temperature range (12.5–15.8°C, Verant et al. 2012) for *P. destructans* growth (Caire et al. 2019).

The true year of *P. destructans* arrival at some sites in central Texas is likely earlier than the designation in our model, as some of them had relatively high prevalence the first year the sites were sampled (Figures 1.7, S1). By including latitude and both latitude and longitude as covariates in our model selection for the *P. subflavus* analysis, we were able to conclude that whether the samples were collected in Texas or not was a better predictor for *P. destructans* prevalence, suggesting there is something about the different patterns of pathogen progression that is unique to Texas. However, given that the Texas samples were the furthest south and west of the two datasets and that this is the furthest southwest extent of *P. subflavus*' range in the US, there could be a "southwestern effect" on *P. destructans* invasion dynamics (Figure S2). The

inclusion of additional *P. subflavus* samples in the southeast US could further elucidate the spatial dynamics of *P. destructans* invasion in North America and demonstrate that these trends are more of a North vs. South difference (i.e., latitudinal) than East vs. West.

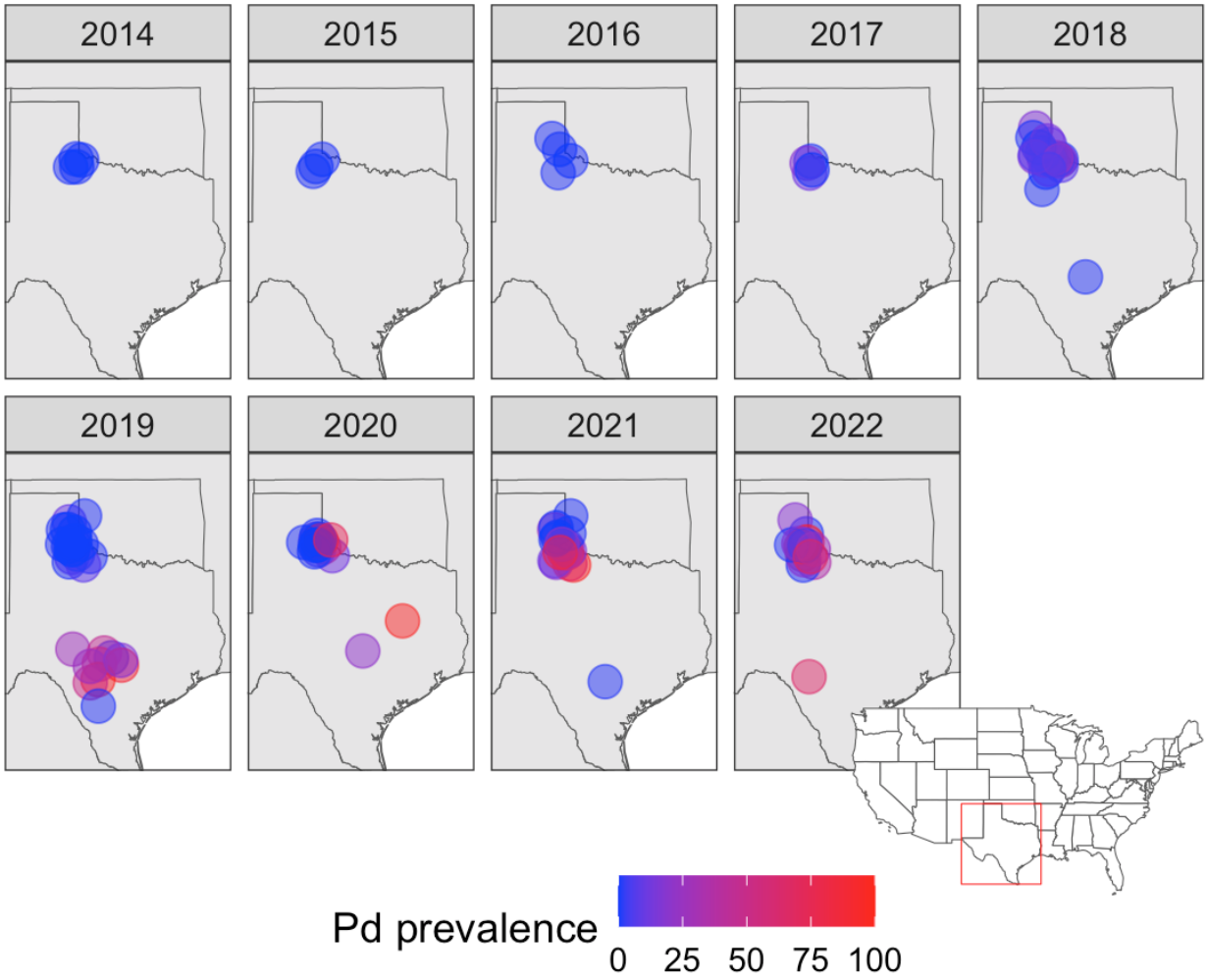

Figure 1.7. *Pseudogymnoascus destructans* spread map by sampling year (vertical panels) across all sites where *M. velifer* were sampled in Texas. *P. destructans* prevalence increases at sites in heat map colors from low (blue) to high (red).

Microbial skin assemblages, particularly yeast diversity and abundance, are strongly associated with WNS resistance in eastern bats (Vanderwolf et al. 2021a). Recent models based on bat skin fungal assemblages predicted WNS susceptibility in 13 western bat species and found only one species, *Myotis velifer*, predicted to be WNS resistant (Vanderwolf et al. 2021b). These

differences in microbial skin assemblages could be a reason for the different infection dynamics we found in *M. velifer*, although we do still see increases in *P. destructans* prevalence over time in this species. The emergence of the disease in Texas *M. velifer* (Texas Parks and Wildlife Department 2020) indicates the species is still susceptible to WNS.

Infectious fungal diseases are one of the leading threats to wildlife today (Fisher et al. 2020). The global chytridiomycosis panzootic in amphibians exemplifies the dangers of rapid pathogen spread and the fragility of wildlife health in the face of modern globalization (Fisher and Garner, 2020). Wildlife pathogens are also an important public health issue from a One Health perspective as we learned from the global COVID-19 pandemic (Ferri & Lloyd-Evans 2021). The rapid spread of *P. destructans* across North America and the resulting widespread declines of hibernating bat species has created an urgent need for research into the host-pathogen dynamics of WNS and effective conservation measures in response to the threat.

The first step of understanding differential disease outcomes in host populations is establishing if there are differences in disease dynamics across populations and regions. This study identifies key differences in the patterns of *P. destructans* invasion between bats in Texas and the eastern and midwestern US. While these different pathogen dynamics appear to be slowing or delaying disease in Texas, it is evident that these bats are still susceptible to WNS and are under serious threat. The unique diversity and abundance of bat species in Texas makes it an important area for further study into the long-term host and pathogen dynamics of WNS. The invasion of *P. destructans* into the range of large hibernating *M. velifer* colonies in Texas and the arid Southwest (some of which intermingle in caves with migratory species) demonstrates the

potential for the pathogen to continue to spread and invade naïve bat populations across the southern extent of North America and beyond.

CHAPTER THREE: Investigating the spatiotemporal dynamics of *Pseudogymnoascus destructans* invasion in the U.S. Southwest

INTRODUCTION

The rapid spread of cold-adapted fungal pathogens is one of the leading threats to wildlife amid modern globalization (Fisher and Garner 2020). In North America, hibernating bats are experiencing unprecedented declines from an infectious fungal disease called white-nose syndrome (WNS; Frick et al. 2010, 2017). The causative agent, *Pseudogymnoascus destructans*, is a fungal pathogen that parasitizes bats during hibernation, causing characteristic lesions on the muzzle and wing membranes of infected bats (Meteyer et al. 2009). The disease disrupts the physiological homeostasis of infected bats by causing epidermal tissue damage resulting in water and electrolyte imbalances, more frequent arousals from torpor during hibernation, and depletion of crucial fat reserves (Reeder et al. 2012, Cryan et al. 2013, Warnecke et al. 2013, Verant et al. 2014).

The impacts of WNS have been studied extensively in the eastern and midwestern US where most of the mortality has occurred. However, the pathogen continues to spread across the continent into new bat populations and habitats. The implications of the recent arrival of *P. destructans* in the western US, where bat communities are more diverse, are a rapidly growing field of research but are still largely understudied (Hoyt et al. 2021). In addition, the uncertain impacts of climate change compounded with the threat of WNS makes it difficult to predict the future conditions of western bat populations (McClure et al. 2022).

Environmental factors such as temperature and humidity are strong predictors for *P. destructans* growth (Verant et al. 2012, Marroquin et al. 2017). Despite common misconceptions about

hibernacula in the Southwest, many sites are cold and humid enough to support the growth of *P. destructans* (Torres-Cruz et al. 2019). Monitoring bat populations that hibernate in microclimates that are suitable for *P. destructans* growth is critical for early detection of the pathogen. Many bat species rarely show visual signs of WNS, and the use of quantitative PCR (qPCR) testing can provide significantly earlier detection of *P. destructans* than visual surveys alone (Janicki et al. 2015). Investigating infection dynamics during the invasion and establishment of the pathogen allows us to better understand the variable impacts of disease on host populations and identify potential mechanisms of host resistance (Frick et al. 2017).

For many places in the world, bat hibernacula (i.e., winter refuges for dormant bats) consist of very large colonies of bats. For example, bats in the East and Midwestern U.S. hibernate in densely populated caves with bats numbering in the tens of thousands to hundreds of thousands (Bernard and McCracken 2017). In contrast, typical hibernation behavior of western bats is quite different with bats hibernating individually or in small groups of 2–4 individuals (Olson and Barclay 2013). Physical contact between western bats during winter is often limited due to small, isolated hibernating groups (Fenton and Barclay 1980). However, there are still many large colonies of hibernating bats in the West that are potentially susceptible to WNS, particularly in the caves of the Southwestern U.S. (Hayward 1961). The over-wintering behavior of western bats may reduce their risk of *P. destructans* transmission, but also presents numerous challenges to studying the bats themselves and the spread of the disease in the West (Weller et al. 2018).

Our study is the first to document the spread of *P. destructans* across the U.S. Southwest. We investigated the spatiotemporal dynamics of *P. destructans* invasion in the Southwest to examine

the following questions: 1) Where is *P. destructans* in the Southwest? 2) When, by years since detection and by season, is *P. destructans* prevalent? 3) On what species is *P. destructans* detected and on which species is the pathogen most prevalent?

METHODS

Overview

We investigated the spatiotemporal dynamics of *P. destructans* invasion in the Southwestern U.S. by analyzing pathogen prevalence in bat swab samples, guano, and hibernacula environmental samples collected across the region. We used generalized linear mixed-effects models to evaluate the relationship between *P. destructans* presence/absence and bat species, relative *M. velifer* abundance, and years since pathogen detection across the Southwest.

Study Area

From 2018 to 2022, we sampled bat populations for *P. destructans* at 126 sites in four states (New Mexico, Arizona, Nevada, and California) across the Southwest region of the U.S. (Figure 3.1), including but not limited to El Malpais National Monument (ELMA), Carlsbad Caverns National Park (CAVE), Fort Stanton-Snowy River Cave National Conservation Area, Grand Canyon National Park (GRCA), and Grand Canyon-Parashant National Monument (PARA). Sampling began in late winter/early spring and continued through early summer. Sampling sites consisted of caves, mines, and man-made structures that are used by bats as roosting sites. We also captured bats on the landscape with mist-nets at certain sites. Sampling was conducted as minimally invasive as possible to minimize disturbance to the animals and USFWS bat handling protocol for COVID-19 was strictly followed to minimize the risk of infecting the already threatened populations. We strictly adhered to the National White-nose Syndrome

Decontamination Protocol to minimize the risk of our research activities contributing to the spread of *P. destructans*. The Southwest dataset used in this study contains additional *P. destructans* surveillance data that were collected and contributed to this project by collaborators across the region.

Data collection

Both bat and environmental samples were collected using a standardized swabbing protocol (Frick et al. 2017). We collected bat swab samples by dipping a sterile polyester swab in molecular grade sterile water and rubbing it across both the bat's muzzle and forearm 5 times (Langwig et al. 2015a). We collected environmental samples by using a sterile polyester swab that has been dipped in sterile water to swirl along the substrate surface in close proximity to the sampled bat. Swabs were stored in 2 mL sterile cryovials in RNAlater from the field to the lab and stored at -20°C until they were processed. DNA from bat and substrate samples were extracted using DNeasy Blood and Tissue extraction kits (Qiagen, Valencia, CA) with a modification for fungal extractions to include lyticase in addition to proteinase K and buffer ATL during the lysis step (Shuey et al. 2014). We tested for the presence and quantity of *P. destructans* DNA following the Muller et al. (2013) protocol, using real-time quantitative PCR (qPCR). Each sample was tested in duplicate and considered positive for *P. destructans* if at least one qPCR run amplified below a cycle threshold (C_t) of 40 (Frick et al. 2017).

Statistical analyses

We used generalized linear mixed-effects models to examine *P. destructans* prevalence dynamics. We conducted stepwise model comparisons based on Akaike's Information Criterion (AIC; Anderson and Burnham 2002), fitting *P. destructans* surveillance data to a binomial

distribution. We incrementally increased model complexity as predictor variables were added to identify the best-supported model. Predictors included as covariates in the model selection were species, years since *P. destructans* detection (transformed as inverse), sampling location (hibernacula or landscape), time of year (month), colony size, and relative *M. velifer* colony size (greater or less than 1,000), with site as a random effect. The best-supported model for predicting *P. destructans* prevalence in the Southwest included the following covariates: species, years since detection, and relative number of *M. velifer*. Month and sampling location were not among the predictors in the best-fit model. Out of 20 sampled species, the best-supported model was unable to estimate a coefficient for five species (*Idionycteris phyllotis*, *Lasiurus blossevillii*, *Lasionycteris cinereus*, *Myotis auriculus*, and *M. evotis*), likely because there were fewer than 10 samples for each of these species. We also ran a second set of model comparisons based on AIC criteria to determine if overall colony size (for all species) or rough categories of *M. velifer* colony size (greater or less than 1,000) was a better predictor of *P. destructans* prevalence. The resulting best-supported model indicated relative *M. velifer* colony size to be a better predictor of *P. destructans* prevalence than overall colony size. We fit the mixed effects models using R (version 4.0.2) with package glmmTMB.

RESULTS

Species-level examination of P. destructans prevalence

A total of 1,140 samples were collected from 21 different bat species across 126 unique sites in the Southwest. The first year of *P. destructans* detection in the Southwest was 2018 when multiple low-level positives were detected across sites in New Mexico (Figure 2.1). After initial detection, every year sampled produced more positive detections of the pathogen across the

region (Figure 2.1). We detected *P. destructans* in a total of 171 samples (including low-level positives with C_t values of 37–40) across 13 southwestern species (Table 4). For all species with at least 15 samples, raw prevalence values ranged from 1% to 34%. Out of 10 species sampled at

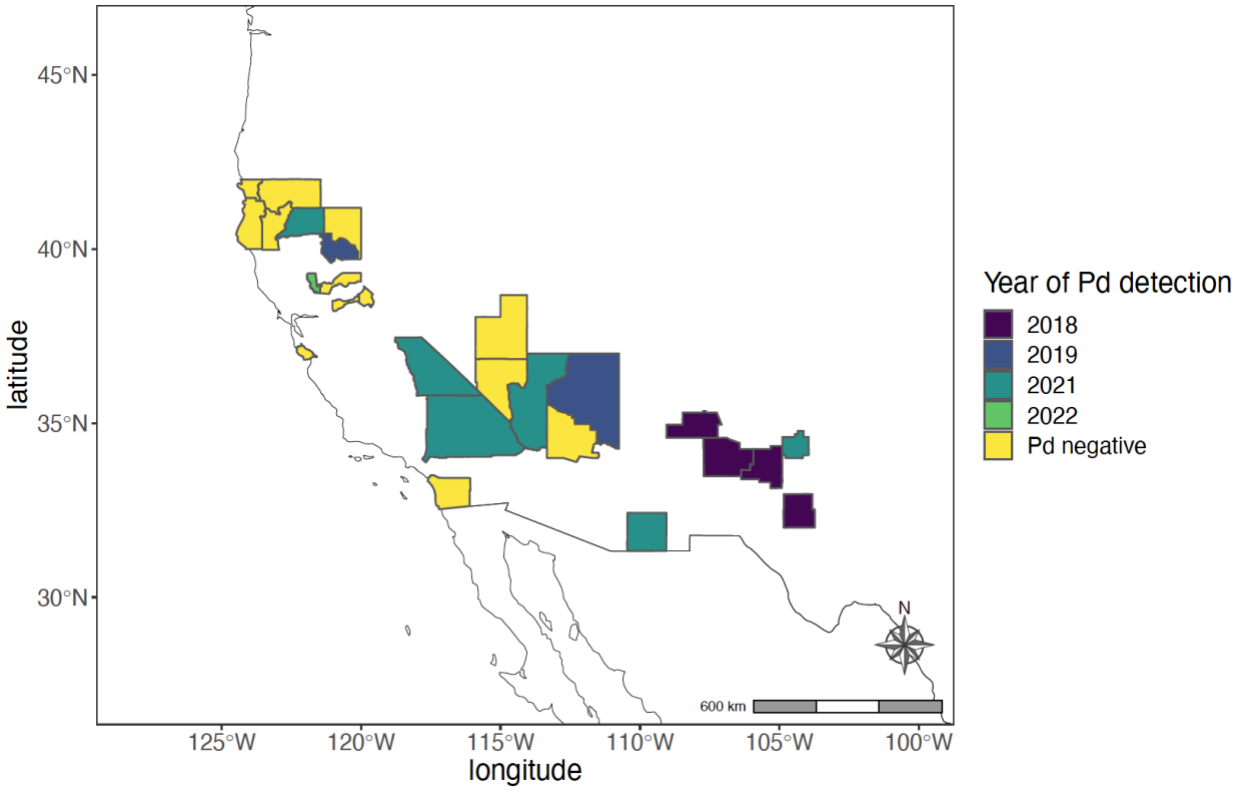

Figure 2.1. Map of *Pseudogymnoascus destructans* arrival in the US Southwest by county. Each county shows where samples were collected and is colored by the year of *P. destructans* arrival.

hibernacula; 7 different species tested positive for *P. destructans* (Table 4). Although, the three negative species from hibernacula had less than 3 samples per species. A total of 19 species were sampled on the landscape by mist-netting with positive detections in 14 species (3 species from the landscape that tested negative had fewer than 10 samples). Interestingly, 11 low-level positives (C_t values of 37–40) were detected in *Antrozous pallidus*, a species whose WNS status is unknown.

Table 4. *Pseudogymnoascus destructans presence/absence by species and sampling method*
Species testing positive (+) or negative (-) for *P. destructans* when sampled at hibernacula or on the landscape. Sample sizes are in parentheses. NA indicates the species was not sampled using that method.

species	hibernacula	landscape
MYVE	+ (79)	+ (73)
ANPA	+ (25)	+ (72)
COTO	+ (90)	+ (28)
EPFU	+ (9)	+ (72)
IDPH	NA	- (6)
LABL	NA	- (4)
LACI	NA	- (13)
LANO	- (1)	+ (26)
MYAU	NA	- (9)
MYCA	- (1)	+ (105)
MYCI	+ (55)	- (27)
MYEV	- (2)	NA
MYLU	NA	+ (123)
Myotis	NA	+ (5)
MYTH	+ (13)	+ (77)
MYVO	+ (7)	+ (32)
MYYU	NA	+ (39)
MYYU/LU	NA	+ (41)
PAHE	NA	+ (54)
TABR	NA	+ (63)

P. destructans impacts in Myotis velifer in the Southwest

Of the 17 total bat species sampled, *P. destructans* prevalence was highest in *M. velifer* (N = 152). At two sites in New Mexico with large *M. velifer* colonies (greater than 1,000 bats), prevalence increased from low (0%) to high (near 100%) in *M. velifer* within 3 years since *P. destructans* detection (Figure 2.2). At the two New Mexico sites with greater than 1,000 *M. velifer*, 4 other species (*Corynorhinus townsendii*, *Antrozous pallidus*, *Myotis thysanodes*, and *Eptesicus fuscus*) all had significantly higher *P. destructans* prevalence than at sites with fewer than 1,000 *M. velifer* (Figure 2.2). For all other samples, whether taken at hibernacula or by mist-nets on the landscape, *P. destructans* prevalence remained low (below 50%) and did not increase with years since detection (Figure 2.2).

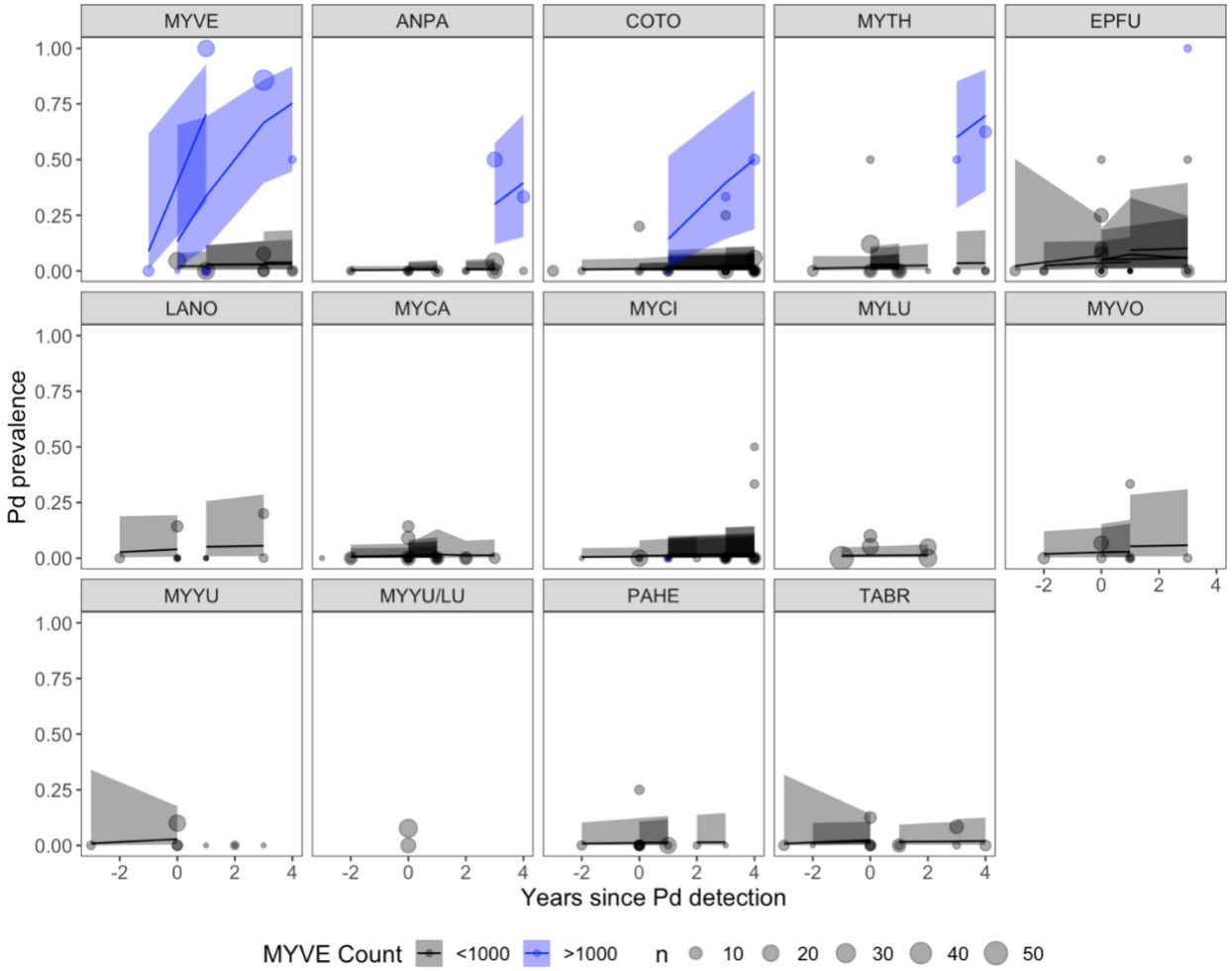

Figure 2.2. *Pseudogymnoascus destructans* prevalence in the Southwest by years since detection by species. Pd prevalence over time is plotted for each site with lines fit from the best-supported model with 95% credible intervals (shaded areas). Pd prevalence from raw data by site and species are plotted as points, with size of the point scaled to the number of samples taken. Sites with greater than 1000 *M. velifer* are plotted (blue) alongside sites with fewer than 1000 *M. velifer* (black).

Seasonal detection of P. destructans

Positive *P. destructans* detections occurred in all seasons that were sampled including late winter (March), spring (April-May), and in the summer (June-July, Figure 2.3). Sampling month was not a significant predictor for *P. destructans* presence/absence as prevalence did not differ between winter, spring, and summer (Figure 2.3). Prevalence was generally low across seasons except at the sites with large *M. velifer* colonies (Figure 2.3). At sites with greater than 1,000 *M.*

velifer, prevalence in year 3 since initial detection was at equally high levels in spring (April) and summer (July) (Figure 2.3).

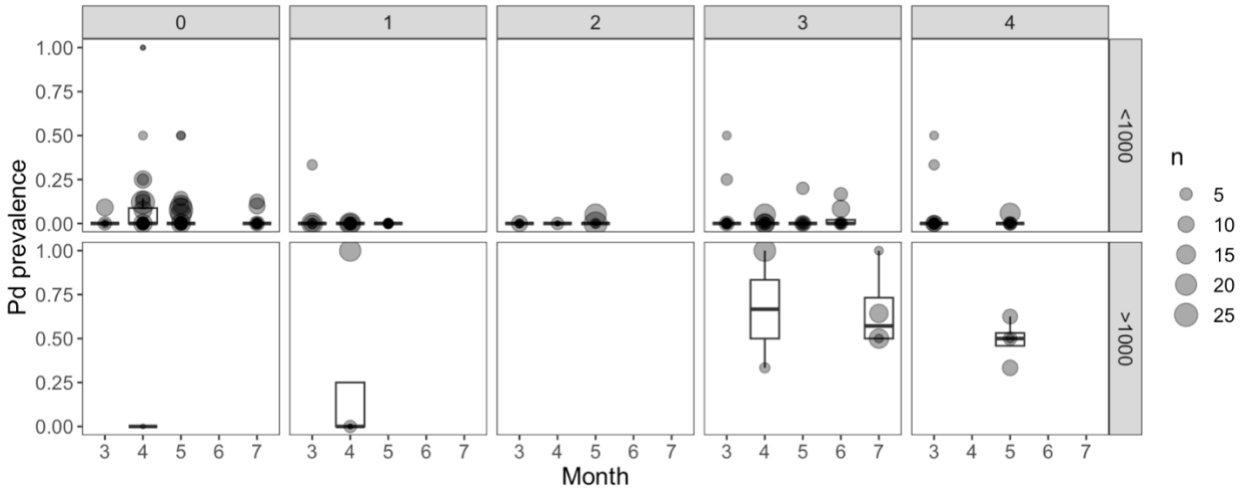

Figure 2.3. *Pseudogymnoascus destructans* prevalence by month with panels (labelled 0–4) representing years since Pd detection. Boxplot shows the spread of data and points represent Pd prevalence by site, species, and date; size of points are scaled to number of samples taken. Top row represents sites with fewer than 1000 *M. velifer* and bottom row represents sites with greater than 1000 *M. velifer*.

DISCUSSION

Pseudogymnoascus destructans appears to be ubiquitous across most bat species in the Southwest, but at low prevalence. Low-level detections of the pathogen were found in many places across the Southwest not indicated on the WNS map from USFWS (Figure 2.1, US Fish and Wildlife Service, 2022). We also found evidence for the presence of *P. destructans* on *A. pallidus*, a species whose WNS status is unknown thus far. Although, 10 out of the 11 low-level positive detections on *A. pallidus* were associated with a single cave in New Mexico that harbors a large hibernating *M. velifer* colony and a large *M. thysanodes* maternity colony.

The pathogen invasion dynamics at 2 caves in New Mexico with large hibernating *M. velifer* colonies were significantly different from all other southwestern sites sampled in the study. *P.*

destructans prevalence increased over time at these sites in multiple species in addition to *M. velifer*, the species reaching the highest prevalence near 100% (Figure 2.2). At these 2 sites, relatively high *P. destructans* prevalence was also found in *A. pallidus*, *C. townsendii*, *M. thysanodes*, and *E. fuscus* (Figure 2.2). *Corynorhinus townsendii* has been documented with *P. destructans* but has not been found exhibiting WNS symptoms (US Fish and Wildlife Service, 2022). *Myotis thysanodes* and *E. fuscus* have both been documented with diagnostic signs of WNS, but with little to no mortality (US Fish and Wildlife Service, 2022). For these species, *P. destructans* prevalence was low at all other southwestern sites in the study. Interestingly, for sites with fewer than 1,000 *M. velifer*, *P. destructans* was detected at equally low prevalence for bats sampled by mist-netting on the landscape and those sampled at hibernacula.

Our results suggest *Myotis velifer* is currently a key species in the invasion and transmission of *P. destructans* in the Southwest. We found evidence for similar annual patterns of *P. destructans* progression in *M. velifer* in Texas and New Mexico. We were unable to make temporal predictions within-hibernation because we were only able to sample hibernacula once at the end of hibernation. However, *M. velifer* in New Mexico exhibit similar clustering behavior and roost preferences to Texas populations. In April of 2021, at one of the large *M. velifer* colonies in New Mexico, we found the fungus growing all over the muzzles of many cave bats indicating that not only are New Mexico *M. velifer* susceptible to WNS, but the disease is likely already occurring in the state.

Due to the COVID-19 pandemic and related federal restrictions on bat research activities, many sites were unable to be sampled in 2020. This left an unfortunate gap in our dataset during a

critical period of the invasion of *P. destructans* in the Southwest. However, despite the holes in our dataset, we were still able to identify important patterns of *P. destructans* prevalence during its invasion and establishment in the region. The results of this study highlight the importance of continued surveillance for *P. destructans* in the region, the appropriate methods for early detection of the pathogen, and the need for monitoring host populations for signs of WNS.

Compared to the Texas and eastern US, we see different species composition within hibernacula and across the region, greater species diversity compared to the East, differences in hibernation ecology and behavior, and different sampling methods. Moreover, much of the winter behavior of western bats is still unknown. These fundamental differences make comparative analyses across regions difficult. In this study, we were able to document important host and pathogen dynamics of *P. destructans* during its invasion and establishment in the Southwest. Further study of the disease dynamics of WNS is needed to better understand the long-term implications of *P. destructans* in the West.

REFERENCES

Alves, D. M. C. C., Terribile, L. C., & Brito, D. (2014). The potential impact of white-nose syndrome on the conservation status of North American bats. *PLoS ONE*, *9*(9), e107395. https://doi.org/10.1371/journal.pone.0107395

Ammerman LK, Hice CL, Schmidly DJ. (2012). Bats of Texas. College Station, TX: *Texas A&M University Press.*

Anderson, D. R., & Burnham, K. P. (2002). Avoiding pitfalls when using information-theoretic methods. *The Journal of Wildlife Management*, *66*(3), 912. https://doi.org/10.2307/3803155

Ange-Stark, M., Cheng, T. L., Hoyt, J. R., Langwig, K. E., Parise, K. L., Frick, W. F., Kilpatrick, A. M., MacManes, M. D., & Foster, J. T. (2019). White-nose syndrome restructures bat skin microbiomes. bioRxiv. https://doi.org/10.1101/614842

Auteri, G. G., & Knowles, L. L. (2020). Decimated little brown bats show potential for adaptive change. *Scientific Reports*, *10*(1), 3023. https://doi.org/10.1038/s41598-020-59797-4

Bernard, R. F., & McCracken, G. F. (2017). Winter behavior of bats and the progression of white-nose syndrome in the southeastern United States. *Ecology and Evolution*, *7*(5), 1487–1496. https://doi.org/10.1002/ece3.2772

Blehert, D. S., Hicks, A. C., Behr, M., Meteyer, C. U., Berlowski-Zier, B. M., Buckles, E. L., Coleman, J. T. H., Darling, S. R., Gargas, A., Niver, R., Okoniewski, J. C., Rudd, R. J., & Stone, W. B. (2009). Bat white-nose syndrome: an emerging fungal pathogen? *Science*, *323*(5911), 227–227. https://doi.org/10.1126/science.1163874

Caire, W., Loucks, L. S., Shaw, J. B., Evans, J. W., Gillies, K. E., & Caywood, M. A. (2019). Variation in the number of hibernating cave myotis (*Myotis velifer*) in western Oklahoma and northwest Texas caves prior to the arrival of white-nose syndrome *The Southwestern Naturalist*, *63*(2), 124. https://doi.org/10.1894/0038-4909-63-2-124

Cable, A. B., Willcox, E. V., & Leppanen, C. (2022). Contaminant exposure as an additional stressor to bats affected by white-nose syndrome: Current evidence and knowledge gaps. *Ecotoxicology*, *31*(1), 12–23. https://doi.org/10.1007/s10646-021-02475-6

Cheng, T. L., Reichard, J. D., Coleman, J. T. H., Weller, T. J., Thogmartin, W. E., Reichert, B. E., Bennett, A. B., Broders, H. G., Campbell, J., Etchison, K., Feller, D. J., Geboy, R., Hemberger, T., Herzog, C., Hicks, A. C., Houghton, S., Humber, J., Kath, J. A., King, R. A., … Frick, W. F. (2021). The scope and severity of white-nose syndrome on hibernating bats in North America. *Conservation Biology*, *35*, 1586–1597. https://doi.org/10.1111/cobi.13739

Cheng, T. L., Gerson, A., Moore, M. S., Reichard, J. D., DeSimone, J., Willis, C. K. R., Frick, W. F., & Kilpatrick, A. M. (2019). Higher fat stores contribute to persistence of little brown

bat populations with white-nose syndrome. *Journal of Animal Ecology*, *88*(4), 591–600. https://doi.org/10.1111/1365-2656.12954

Cheng, T. L., Mayberry, H., McGuire, L. P., Hoyt, J. R., Langwig, K. E., Nguyen, H., Parise, K. L., Foster, J. T., Willis, C. K. R., Kilpatrick, A. M., & Frick, W. F. (2017). Efficacy of a probiotic bacterium to treat bats affected by the disease white-nose syndrome. *Journal of Applied Ecology*, *54*(3), 701–708. https://doi.org/10.1111/1365-2664.12757

Cryan, P. M., Meteyer, C. U., Blehert, D. S., Lorch, J. M., Reeder, D. M., Turner, G. G., Webb, J., Behr, M., Verant, M., Russell, R. E., & Castle, K. T. (2013). Electrolyte depletion in white-nose syndrome bats. *Journal of Wildlife Diseases*, *49*(2), 398–402. https://doi.org/10.7589/2012-04-121

Drees, K. P., Lorch, J. M., Puechmaille, S. J., Parise, K. L., Wibbelt, G., Hoyt, J. R., Sun, K., Jargalsaikhan, A., Dalannast, M., Palmer, J. M., Lindner, D. L., Marm Kilpatrick, A., Pearson, T., Keim, P. S., Blehert, D. S., & Foster, J. T. (2017). Phylogenetics of a fungal invasion: origins and widespread dispersal of white-nose syndrome. *MBio*, *8*(6). https://doi.org/10.1128/mBio.01941-17

Fenton, M. B., & Barclay, R. M. R. (1980). *Myotis lucifugus*. *Mammalian Species*, *142*, 1. https://doi.org/10.2307/3503792

Ferri, M., & Lloyd-Evans, M. (2021). The contribution of veterinary public health to the management of the COVID-19 pandemic from a One Health perspective. *One Health*, *12*, 100230. https://doi.org/10.1016/j.onehlt.2021.100230

Field, K. A., Johnson, J. S., Lilley, T. M., Reeder, S. M., Rogers, E. J., Behr, M. J., & Reeder, D. M. (2015). The white-nose syndrome transcriptome: activation of anti-fungal host responses in wing tissue of hibernating little brown Myotis. *PLoS Pathogens*, *11*(10), e1005168. https://doi.org/10.1371/journal.ppat.1005168

Fisher, M. C., & Garner, T. W. J. (2020). Chytrid fungi and global amphibian declines. *Nature Reviews Microbiology*, *18*(6), 332–343. https://doi.org/10.1038/s41579-020-0335-x

Fisher, M. C., Gurr, S. J., Cuomo, C. A., Blehert, D. S., Jin, H., Stukenbrock, E. H., Stajich, J. E., Kahmann, R., Boone, C., Denning, D. W., Gow, N. A. R., Klein, B. S., Kronstad, J. W., Sheppard, D. C., Taylor, J. W., Wright, G. D., Heitman, J., Casadevall, A., & Cowen, L. E. (2020). Threats posed by the fungal kingdom to humans, wildlife, and agriculture. *mBio*, *11*(3). https://doi.org/10.1128/mBio.00449-20

Fletcher, Q. E., Webber, Q. M. R., & Willis, C. K. R. (2020). Modelling the potential efficacy of treatments for white-nose syndrome in bats. *Journal of Applied Ecology*, *57*(7), 1283–1291. https://doi.org/10.1111/1365-2664.13619

Forsythe, A., Giglio, V., Asa, J., & Xu, J. (2018). Phenotypic divergence along geographic gradients reveals potential for rapid adaptation of the white-nose syndrome pathogen,

Pseudogymnoascus destructans, in North America. Applied and Environmental Microbiology, 84(16). https://doi.org/10.1128/AEM.00863-18

Frick, W. F., Cheng, T. L., Langwig, K. E., Hoyt, J. R., Janicki, A. F., Parise, K. L., Foster, J. T., & Kilpatrick, A. M. (2017). Pathogen dynamics during invasion and establishment of white-nose syndrome explain mechanisms of host persistence. *Ecology*, *98*(3), 624–631. https://doi.org/10.1002/ecy.1706

Frick, W. F., Puechmaille, S. J., Hoyt, J. R., Nickel, B. A., Langwig, K. E., Foster, J. T., Barlow, K. E., Bartonička, T., Feller, D., Haarsma, A.-J., Herzog, C., Horáček, I., van der Kooij, J., Mulkens, B., Petrov, B., Reynolds, R., Rodrigues, L., Stihler, C. W., Turner, G. G., & Kilpatrick, A. M. (2015). Disease alters macroecological patterns of North American bats: Disease alters macroecology of bats. *Global Ecology and Biogeography*, *24*(7), 741–749. https://doi.org/10.1111/geb.12290

Frick, W. F., Pollock, J. F., Hicks, A. C., Langwig, K. E., Reynolds, D. S., Turner, G. G., Butchkoski, C. M., & Kunz, T. H. (2010). An emerging disease causes regional population collapse of a common North American bat species. *Science*, *329*(5992), 679–682. https://doi.org/10.1126/science.1188594

Hayward, B. J. (1961). The Natural History of the Cave Bat, *Myotis velifer*. *The University of Arizona ProQuest Dissertations Publishing*, 130 pp.

Hicks, A. C., Darling, S., Flewelling, J., von Linden, R., Meteyer, C. U., Redell, D., White, J. P., Redell, J., Smith, R., Blehert, D., Rayman, N., Hoyt, J. R., Okoniewski, J. C., & Langwig, K. E. (2021). Environmental transmission of *Pseudogymnoascus destructans* to hibernating little brown bats. *Ecology*. https://doi.org/10.1101/2021.07.01.450774

Hoyt, J. R., Kilpatrick, A. M., Langwig, K. E. (2021). Ecology and impacts of white-nose syndrome on bats. *Nature Reviews Microbiology*, *19*(3). https://doi.org/10.1038/s41579-020-00493-5

Hoyt, J. R., Langwig, K. E., White, J. P., Kaarakka, H. M., Redell, J. A., Kurta, A., DePue, J. E., Scullon, W. H., Parise, K. L., Foster, J. T., Frick, W. F., & Kilpatrick, A. M. (2018). Cryptic connections illuminate pathogen transmission within community networks. *Nature*, *563*(7733), 710–713. https://doi.org/10.1038/s41586-018-0720-z

Hoyt, J. R., Cheng, T. L., Langwig, K. E., Hee, M. M., Frick, W. F., & Kilpatrick, A. M. (2015b). Bacteria isolated from bats inhibit the growth of *Pseudogymnoascus destructans*, the causative agent of White-Nose Syndrome. *PLOS ONE*, *10*(4), e0121329. https://doi.org/10.1371/journal.pone.0121329

Hoyt, J. R., Langwig, K. E., Okoniewski, J., Frick, W. F., Stone, W. B., & Kilpatrick, A. M. (2015a). Long-Term persistence of *Pseudogymnoascus destructans*, the causative agent of White-Nose Syndrome, in the absence of bats. *EcoHealth*, *12*(2), 330–333. https://doi.org/10.1007/s10393-014-0981-4

Hoyt, J. R., Langwig, K. E., Sun, K., Lu, G., Parise, K. L., Jiang, T., Frick, W. F., Foster, J. T., Feng, J., & Kilpatrick, A. M. (2016). Host persistence or extinction from emerging infectious disease: Insights from white-nose syndrome in endemic and invading regions. *Proceedings of the Royal Society B: Biological Sciences*, *283*(1826), 20152861. https://doi.org/10.1098/rspb.2015.2861

Hoyt, J. R., Langwig, K. E., White, J. P., Kaarakka, H. M., Redell, J. A., Parise, K. L., Frick, W. F., Foster, J. T., & Kilpatrick, A. M. (2019). Field trial of a probiotic bacteria to protect bats from white-nose syndrome. *Scientific Reports*, *9*(1), 9158. https://doi.org/10.1038/s41598-019-45453-z

Hoyt, J. R., Sun, K., Parise, K. L., Lu, G., Langwig, K. E., Jiang, T., Yang, S., Frick, W. F., Kilpatrick, A. M., Foster, J. T., & Feng, J. (2015). Widespread bat white-nose syndrome fungus, Northeastern China. *Emerging Infectious Diseases*, *22*(1), 140–142. https://doi.org/10.3201/eid2201.151314

Janicki, A. F., Frick, W. F., Kilpatrick, A. M., Parise, K. L., Foster, J. T., & McCracken, G. F. (2015). Efficacy of visual surveys for White-Nose Syndrome at bat hibernacula. *PLOS ONE*, *10*(7), e0133390. https://doi.org/10.1371/journal.pone.0133390

Kunz, T. H., Braun de Torrez, E., Bauer, D., Lobova, T., & Fleming, T. H. (2011). Ecosystem services provided by bats: Ecosystem services provided by bats. *Annals of the New York Academy of Sciences*, *1223*(1), 1–38. https://doi.org/10.1111/j.1749-6632.2011.06004.x

Langwig, K. E., Hoyt, J. R., Parise, K. L., Frick, W. F., Foster, J. T., & Kilpatrick, A. M. (2017). Resistance in persisting bat populations after white-nose syndrome invasion. *Philosophical Transactions of the Royal Society B: Biological Sciences*, *372*(1712), 20160044. https://doi.org/10.1098/rstb.2016.0044

Langwig, K. E., Frick, W. F., Hoyt, J. R., Parise, K. L., Drees, K. P., Kunz, T. H., Foster, J. T., & Kilpatrick, A. M. (2016). Drivers of variation in species impacts for a multi-host fungal disease of bats. *Philosophical Transactions of the Royal Society B: Biological Sciences*, *371*(1709), 20150456. https://doi.org/10.1098/rstb.2015.0456

Langwig, K. E., Frick, W. F., Reynolds, R., Parise, K. L., Drees, K. P., Hoyt, J. R., Cheng, T. L., Kunz, T. H., Foster, J. T., & Kilpatrick, A. M. (2015a). Host and pathogen ecology drive the seasonal dynamics of a fungal disease, white-nose syndrome. *Proceedings of the Royal Society B: Biological Sciences*, *282*(1799), 20142335. https://doi.org/10.1098/rspb.2014.2335

Langwig, K. E., Hoyt, J. R., Parise, K. L., Kath, J., Kirk, D., Frick, W. F., Foster, J. T., & Kilpatrick, A. M. (2015b). Invasion dynamics of white-nose syndrome fungus, Midwestern United States, 2012–2014. *Emerging Infectious Diseases*, *21*(6), 1023–1026. https://doi.org/10.3201/eid2106.150123

Langwig, K. E., Frick, W. F., Bried, J. T., Hicks, A. C., Kunz, T. H., & Marm Kilpatrick, A. (2012). Sociality, density-dependence and microclimates determine the persistence of populations suffering from a novel fungal disease, white-nose syndrome. *Ecology Letters*, *15*(9), 1050–1057. https://doi.org/10.1111/j.1461-0248.2012.01829.x

Lorch, J. M., Palmer, J. M., Lindner, D. L., Ballmann, A. E., George, K. G., Griffin, K., Knowles, S., Huckabee, J. R., Haman, K. H., Anderson, C. D., Becker, P. A., Buchanan, J. B., Foster, J. T., & Blehert, D. S. (2016). First detection of bat white-nose syndrome in Western North America. *mSphere*, *1*(4). https://doi.org/10.1128/mSphere.00148-16

Lorch, J. M., Muller, L. K., Russell, R. E., O'Connor, M., Lindner, D. L., & Blehert, D. S. (2013). Distribution and environmental persistence of the causative agent of white-nose syndrome, *Geomyces destructans*, in bat hibernacula of the Eastern United States. *Applied and Environmental Microbiology*, *79*(4), 1293–1301. https://doi.org/10.1128/AEM.02939-12

Lorch, J. M., Meteyer, C. U., Behr, M. J., Boyles, J. G., Cryan, P. M., Hicks, A. C., Ballmann, A. E., Coleman, J. T. H., Redell, D. N., Reeder, D. M., & Blehert, D. S. (2011). Experimental infection of bats with *Geomyces destructans* causes white-nose syndrome. *Nature*, *480*(7377), 376–378. https://doi.org/10.1038/nature10590

Marroquin, C. M., Lavine, J. O., & Windstam, S. T. (2017). Effect of humidity on development of *Pseudogymnoascus destructans* , the causal agent of bat white-nose syndrome. *Northeastern Naturalist*, *24*(1), 54–64. https://doi.org/10.1656/045.024.0105

McClure, M. L., Hranac, C. R., Haase, C. G., McGinnis, S., Dickson, B. G., Hayman, D. T. S., McGuire, L. P., Lausen, C. L., Plowright, R. K., Fuller, N., & Olson, S. H. (2022). Projecting the compound effects of climate change and white-nose syndrome on North American bat species. *Climate Change Ecology*, *3*, 100047. https://doi.org/10.1016/j.ecochg.2021.100047

McGuire, L. P., Turner, J. M., Warnecke, L., McGregor, G., Bollinger, T. K., Misra, V., Foster, J. T., Frick, W. F., Kilpatrick, A. M., & Willis, C. K. R. (2016). White-nose syndrome disease severity and a comparison of diagnostic methods. *EcoHealth*, *13*(1), 60–71. https://doi.org/10.1007/s10393-016-1107-y

Meierhofer, M. B., Johnson, J. S., Leivers, S. J., Pierce, B. L., Evans, J. E., & Morrison, M. L. (2019). Winter habitats of bats in Texas. *PLOS ONE*, *14*(8), e0220839. https://doi.org/10.1371/journal.pone.0220839

Meierhofer MB, Lilley TM, Ruokolainen L, Johnson JS, Parratt SR, Morrison ML, Pierce BL, Evans JW, Anttila J . (2021). Ten-year projection of white-nose syndrome disease dynamics at the southern leading-edge of infection in North America. *Proceedings of the Royal Society B,* 288: 20210719. https://doi.org/10.1098/rspb.2021.0719

Meteyer, C. U., Buckles, E. L., Blehert, D. S., Hicks, A. C., Green, D. E., Shearn-Bochsler, V., Thomas, N. J., Gargas, A., & Behr, M. J. (2009). Histopathologic criteria to confirm white-nose syndrome in bats. *Journal of Veterinary Diagnostic Investigation*, *21*(4), 411–414. https://doi.org/10.1177/104063870902100401

Muller, L. K., Lorch, J. M., Lindner, D. L., O'Connor, M., Gargas, A., & Blehert, D. S. (2013). Bat white-nose syndrome: A real-time TaqMan polymerase chain reaction test targeting the intergenic spacer region of *Geomyces destructans*. *Mycologia*, *105*(2), 253–259. https://doi.org/10.3852/12-242

Olson, C. R., & Barclay, R. M. R. (2013). Concurrent changes in group size and roost use by reproductive female little brown bats (*Myotis lucifugus*). *Canadian Journal of Zoology*, *91*(3), 149–155. https://doi.org/10.1139/cjz-2012-0267

Puechmaille, S. J., Wibbelt, G., Korn, V., Fuller, H., Forget, F., Mühldorfer, K., Kurth, A., Bogdanowicz, W., Borel, C., Bosch, T., Cherezy, T., Drebet, M., Görföl, T., Haarsma, A.-J., Herhaus, F., Hallart, G., Hammer, M., Jungmann, C., Le Bris, Y., … Teeling, E. C. (2011). Pan-European distribution of white-nose syndrome fungus (*Geomyces destructans*) not associated with mass mortality. *PLoS ONE*, *6*(4), e19167. https://doi.org/10.1371/journal.pone.0019167

Reeder, D. M., Frank, C. L., Turner, G. G., Meteyer, C. U., Kurta, A., Britzke, E. R., Vodzak, M. E., Darling, S. R., Stihler, C. W., Hicks, A. C., Jacob, R., Grieneisen, L. E., Brownlee, S. A., Muller, L. K., & Blehert, D. S. (2012). Frequent arousal from hibernation linked to severity of infection and mortality in bats with white-nose syndrome. *PLoS ONE*, *7*(6), e38920. https://doi.org/10.1371/journal.pone.0038920

Reynolds, H. T., & Barton, H. A. (2014). Comparison of the white-nose syndrome agent *Pseudogymnoascus destructans* to cave-dwelling relatives suggests reduced saprotrophic enzyme activity. *PLoS ONE*, *9*(1), e86437. https://doi.org/10.1371/journal.pone.0086437

Rocke, T. E., Kingstad-Bakke, B., Wüthrich, M., Stading, B., Abbott, R. C., Isidoro-Ayza, M., Dobson, H. E., dos Santos Dias, L., Galles, K., Lankton, J. S., Falendysz, E. A., Lorch, J. M., Fites, J. S., Lopera-Madrid, J., White, J. P., Klein, B., & Osorio, J. E. (2019). Virally-vectored vaccine candidates against white-nose syndrome induce anti-fungal immune response in little brown bats (*Myotis lucifugus*). *Scientific Reports*, *9*(1), 6788. https://doi.org/10.1038/s41598-019-43210-w

Schmidly DJ, Bradley RD. (2016). The Mammals of Texas. Austin, TX: *University of Texas Press.*

Shapiro, H. G., Willcox, A. S., Willcox, E. V., & Verant, M. L. (2021). U.S. National Park visitor perceptions of bats and white-nose syndrome. *Biological Conservation*, *261*, 109248. https://doi.org/10.1016/j.biocon.2021.109248

Shuey, M. M., Drees, K. P., Lindner, D. L., Keim, P., & Foster, J. T. (2014). Highly sensitive quantitative PCR for the detection and differentiation of *Pseudogymnoascus destructans* and other *Pseudogymnoascus* Species. *Applied and Environmental Microbiology*, *80*(5), 1726–1731. https://doi.org/10.1128/AEM.02897-13

Taylor, P. J., Grass, I., Alberts, A. J., Joubert, E., & Tscharntke, T. (2018). Economic value of bat predation services – A review and new estimates from macadamia orchards. *Ecosystem Services*, *30*, 372–381. https://doi.org/10.1016/j.ecoser.2017.11.015

Torres-Cruz, T. J., Porras-Alfaro, A., Caimi, N., Nwabologu, O., Strach, E., Read, K., Young, J., Buecher, D., & Northup, D. (2019). Are microclimate conditions in El Malpais National Monument caves in New Mexico, USA suitable for *Pseudogymnoascus* growth? *International Journal of Speleology*, *48*(2), 191–202. https://doi.org/10.5038/1827-806X.48.2.2254

US Fish and Wildlife Service. White-nose Syndrome Response Team. (2022). White-nose syndrome occurrence map. whitenosesyndrome.org/where-is-wns

Vanderwolf, K. J., Campbell, L. J., Taylor, D. R., Goldberg, T. L., Blehert, D. S., & Lorch, J. M. (2021b). Mycobiome traits associated with disease tolerance predict many Western North American bat species will be susceptible to white-nose syndrome. *Microbiology Spectrum*, *9*(1), e00254-21. https://doi.org/10.1128/Spectrum.00254-21

Vanderwolf, K. J., Campbell, L. J., Goldberg, T. L., Blehert, D. S., & Lorch, J. M. (2021a). Skin fungal assemblages of bats vary based on susceptibility to white-nose syndrome. *The ISME Journal*, *15*(3), 909–920. https://doi.org/10.1038/s41396-020-00821-w

Verant, M. L., Boyles, J. G., Waldrep, W., Wibbelt, G., & Blehert, D. S. (2012). Temperature-dependent growth of *Geomyces destructans*, the fungus that causes bat white-nose syndrome. *PLoS ONE*, *7*(9), e46280. https://doi.org/10.1371/journal.pone.0046280

Verant, M. L., Meteyer, C. U., Speakman, J. R., Cryan, P. M., Lorch, J. M., & Blehert, D. S. (2014). White-nose syndrome initiates a cascade of physiologic disturbances in the hibernating bat host. *BMC Physiology*, *14*(10), 11. https://doi:10.1186/s12899-014-0010-4

Warnecke, L., Turner, J. M., Bollinger, T. K., Misra, V., Cryan, P. M., Blehert, D. S., Wibbelt, G., & Willis, C. K. R. (2013). Pathophysiology of white-nose syndrome in bats: A mechanistic model linking wing damage to mortality. *Biology Letters*, *9*(4), 20130177. https://doi.org/10.1098/rsbl.2013.0177

Weller, T. J., Rodhouse, T. J., Neubaum, D. J., Ormsbee, P. C., Dixon, R. D., Popp, D. L., Williams, J. A., Osborn, S. D., Rogers, B. W., Beard, L. O., McIntire, A. M., Hersey, K. A., Tobin, A., Bjornlie, N. L., Foote, J., Bachen, D. A., Maxell, B. A., Morrison, M. L., Thomas, S. C., … Navo, K. W. (2018). A review of bat hibernacula across the western United States: Implications for white-nose syndrome surveillance and management. *PLOS ONE*, *13*(10), e0205647. https://doi.org/10.1371/journal.pone.0205647

White-nose syndrome confirmed in bats in Texas. *Texas Parks and Wildlife Department.* Retrieved February 10, 2022, from https://tpwd.texas.gov/newsmedia/releases/?req=20200305a

Wilson, M. B., Held, B. W., Freiborg, A. H., Blanchette, R. A., & Salomon, C. E. (2017). Resource capture and competitive ability of non-pathogenic Pseudogymnoascus spp. And P. destructans, the cause of white-nose syndrome in bats. *PLOS ONE*, *12*(6), e0178968. https://doi.org/10.1371/journal.pone.0178968

Wolf, L. K., Meierhofer, M. B., Morrison, M. L., Cairns, D. M., & Lacher, T. E. (2022). Modeling the suitability of Texas karst regions for infection by *Pseudogymnoascus destructans* in bats. Journal of Mammalogy, 103(3), 503–511. https://doi.org/10.1093/jmammal/gyac017

Zukal, J., Bandouchova, H., Brichta, J., Cmokova, A., Jaron, K. S., Kolarik, M., Kovacova, V., Kubátová, A., Nováková, A., Orlov, O., Pikula, J., Presetnik, P., Šuba, J., Zahradníková, A., & Martínková, N. (2016). White-nose syndrome without borders: *Pseudogymnoascus destructans* infection tolerated in Europe and Palearctic Asia but not in North America. *Scientific Reports*, *6*(1), 19829. https://doi.org/10.1038/srep19829

APPENDIX

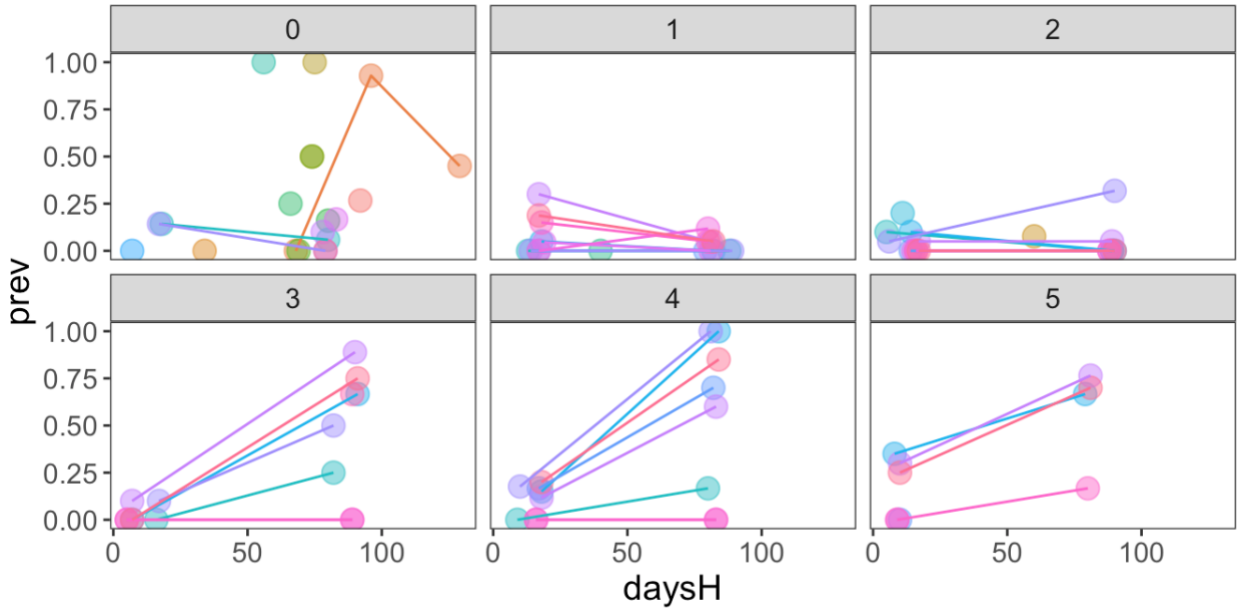

Figure S1. *Pseudogymnoascus destructans* prevalence of *Myotis velifer* at all Texas sites by days in hibernation and years since detection. Raw prevalence values are plotted by site (colors) with prevalence (y-axis) progression shown for each site (lines) by days in hibernation (x-axis) and years since Pd detection (horizontal panels).

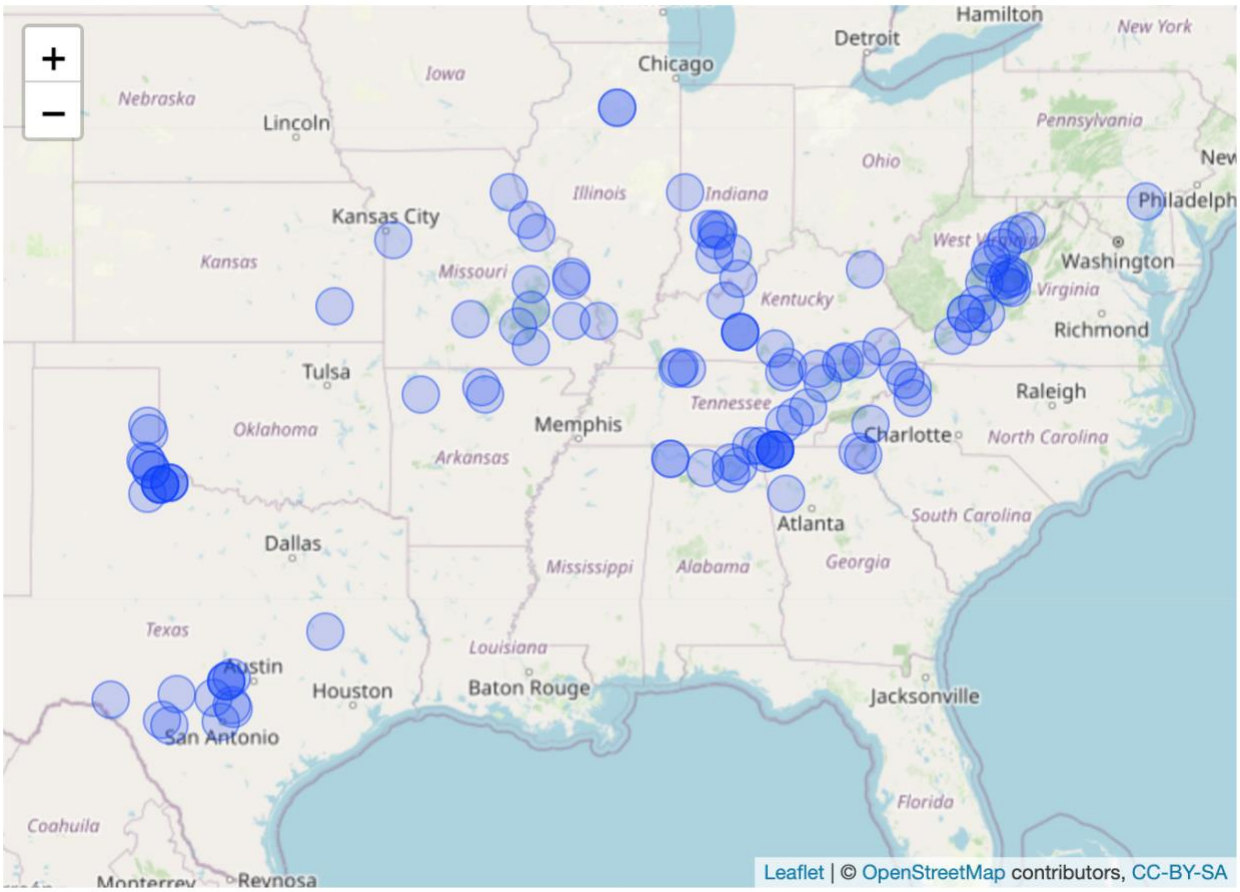

Figure S2: Map of *P. subflavus* sites (data from Frick et al. 2017 with added *P. subflavus* data from Texas.

Table 1. Sample sizes for *Myotis velifer* in Texas versus other. Number of samples and sites for Texas versus those from Frick et al. (2017).

Region	# Samples	# Sites
Other	4367	132
Texas	3014	24
TOTAL	7381	156

Table 2. Sample sizes for *Perimyotis subflavus* in Texas versus other. Number of samples and sites in Texas versus those from Frick et al. (2017).

Region	# Samples	# Sites
Other	1550	89
Texas	1160	17
TOTAL	2710	106

Table 3. Sample sizes by species in the Southwest. Number of samples and number of sites by species.

Species	# Samples	# Sites
Myotis velifer	152	6
Myotis lucifugus	123	3
Corynorhinus townsendii	118	15
Myotis californicus	106	10
Antrozous pallidus	97	10
Myotis thysanodes	90	8
Myotis ciliolabrum	82	14
Eptesicus fuscus	81	14
Tadarida brasiliensis	63	7
Parastresllus hesperus	54	8
Myotis yumanensis/Myotis lucifugus	41	2
Myotis volans	39	4
Myotis yumanensis	39	7
Lasionycteris noctivagans	27	9
Lasionycteris cinereus	13	4
Myotis auriculus	9	1
Lasiurus blossevillii	4	2
Myotis evotis	2	2
TOTAL	1140	126

Table S1. AIC comparisons between models examining *Pseudogymnoascus destructans* presence/absence in *Perimyotis subflavus* by days in hibernation, years since *P. destructans* detection, and Texas (vs. the rest of the species' range) or latitude/longitude.

Model Formula	**df**	**ΔAIC**
r1_ysi + daysHs + texas + daysHs:r1_ysi + texas:r1_ysi + texas:daysHs + (1|site)	8	0
r1_ysi + daysHs + latitude + longitude + daysHs:r1_ysi + latitude:r1_ysi + latitude:daysHs + longitude:r1_ysi + longitude:daysHs + (1|site)	11	0
r1_ysi + daysHs + latitude + daysHs:r1_ysi + latitude:r1_ysi + latitude:daysHs + (1|site)	8	3
r1_ysi + daysHs + daysHs:r1_ysi + (1|site)	5	55

Table S2. Model summary for best-supported model for *Pseudogymnoascus destructans* prevalence in *Perimyotis subflavus* based on AIC comparisons (Table S1).

Variable	**Estimate**	**Std. Error**	**z value**	**p value**
(Intercept)	0.36784646	0.34471994	1.06708787	0.28593216
texastexas	-2.1043225	0.68153074	-3.0876413	0.00201752
r1_ysi	4.9849252	0.52248785	9.5407485	1.42E-21
daysHs	0.6877616	0.17202589	3.99801219	6.39E-05
r1_ysi:daysHs	-0.4902336	0.34343324	-1.4274494	0.1534504
texastexas:daysHs	0.4922107	0.21495985	2.28977973	0.02203409
texastexas:r1_ysi	-3.7210822	0.82215129	-4.5260309	6.01E-06

Table S3. AIC comparisons between models examining *Pseudogymnoascus destructans* presence/absence in southwestern bat species using the following covariates:

1) Year since Pd detection (ysd): we used Pd detection even prior to year 0, the first year of Pd arrival and adjusted the lowest year of Pd detection to zero (e.g., ysd = -3 was adjusted to ysd = 0)
2) Transformed year since pd detection (r1_ysd): ysd was transformed by 1 - (1/(ysd+1)
3) Winter year (wyear): year spanning winter months from November to April where the winter year is the year from January to April; wyear is treated as a discrete (rather than continuous) value
4) Site: spatial location where sampling occurred
5) Sampling location (sampling_location): either hibernacula or landscape
6) Species: bat species sampled
7) MYVE colony size: relative size of *M. velifer* colony, either >1000 bats or <1000 bats
8) month: month sample was taken, month was treated as a discrete (rather than continuous) value

Model Formula	**df**	**ΔAIC**
species + r1_ysd + myve_colony_size + myve_colony_size:r1_ysd + (1|site) + (1|wyear)	25	0
species + r1_ysd + sampling_location + myve_colony_size + myve_colony_size:r1_ysd + (1|site) + (1|wyear)	26	2
species + r1_ysd + sampling_location + myve_colony_size + (1|site) + (1|wyear)	25	3
species + r1_ysd + sampling_location + myve_colony_size + myve_colony_size:r1_ysd + month + (1|site) + (1|wyear)	30	3
species + r1_ysd + sampling_location + myve_colony_size + month + (1|site) + (1|wyear)	29	5
r1_ysd + (1|site) + (1|wyear)	4	24
sampling_location + (1|site) + (1|wyear)	4	24
1 + (1|site) + (1|wyear)	3	25
ysd + (1|site) + (1|wyear)	4	26
species + sampling_location + (1|site) + (1|wyear)	23	29
species + r1_ysd + sampling_location + (1|site) + (1|wyear)	24	31
species + r1_ysd + (1|site) + (1|wyear)	23	33
species + (1|site) + (1|wyear)	22	34
1 + (1|site)	2	52

Table S4. Model summary for best-supported model for *Pseudogymnoascus destructans* prevalence in Southwestern bat species based on AIC comparisons (Table S3).

Variable	**Estimate**	**Std. Error**	**z value**	**p value**
(Intercept)	-4.9112197	2.10835279	-2.3294108	0.01983732
speciesANPA	-1.5385201	0.52832939	-2.9120472	0.00359068
speciesCOTO	-1.0381548	0.62920454	-1.649948	0.09895358
speciesEPFU	0.5386804	0.63005711	0.85497074	0.39256735
speciesIDPH	-12.369253	820.645377	-0.0150726	0.98797427
speciesLABL	-11.804007	830.357934	-0.0142156	0.988658
speciesLACI	-13.257045	913.160238	-0.0145178	0.98841691
speciesLANO	0.62125122	0.8919838	0.69648263	0.48612663
speciesMYAU	-12.649154	843.643844	-0.0149935	0.98803739
speciesMYCA	-1.0437048	0.8792002	-1.1871072	0.23518536
speciesMYCI	-0.9195622	0.8662621	-1.0615288	0.28844964
speciesMYEV	-11.320663	745.592353	-0.0151834	0.98788583
speciesMYLU	-0.6689365	0.83064143	-0.8053252	0.42063205
speciesMyotis	1.22811968	1.26441099	0.97129785	0.33139998
speciesMYTH	-0.3106851	0.62912071	-0.4938402	0.62141901
speciesMYVO	0.29407649	0.90405032	0.32528775	0.7449633
speciesMYYU	-0.4511257	0.95332213	-0.4732144	0.63606026
speciesMYYU/LU	0.71559522	1.13143192	0.63246865	0.52708069
speciesPAHE	-0.9424388	1.14601415	-0.8223623	0.41087072
speciesTABR	-0.5839286	0.8797323	-0.6637572	0.50684573
r1_ysd_altered	1.98915336	2.61336019	0.7611478	0.44656879
myveCount>1000	-15.226159	9.70422775	-1.5690233	0.11664251
r1_ysd_altered:myveCount>1000	23.3800722	11.7849841	1.98388662	0.04726848

Table S5. Second set of AIC comparisons between models asking whether colony size (for all/any species) or just *Myotis velifer* count (split in very rough categories of greater or less than 1000 MYVE) was a better predictor of *Pseudogymnoascus destructans* prevalence in the Southwest.

Model Formula	**df**	**∆AIC**
species + myve_colony_size + r1_ysd + (1|site) + (1|wyear)	13	0
species + r1_ysd + myve_colony_size + myve_colony_size:r1_ysd + (1|site) + (1|wyear)	14	1
species + colony_size + myve_colony_size + r1_ysd + (1|site) + (1|wyear)	14	2
species + r1_ysd + myve_colony_size + myve_colony_size:r1_ysd month + (1|site) + (1|wyear)	18	3
myve_colony_size + (1|site) + (1|wyear)	4	6
species + r1_ysd + myve_colony_size + month + (1|site) + (1|wyear)	17	7
species + colony_size + r1_ysd + colony_size:r1_ysd + (1|site) + (1|wyear)	14	8
species + colony_size + r1_ysd + colony_size:r1_ysd + month (1|site) + (1|wyear)	18	8
species + colony_size + r1_ysd + (1|site) + (1|wyear)	13	9
species + r1_ysd + (1|site) + (1|wyear)	12	11
r1_ysd + (1|site) + (1|wyear)	4	12
species + colony_size + r1_ysd + month + (1|site) + (1|wyear)	17	12
species + colony_size + (1|site) + (1|wyear)	12	17
species + (1|site) + (1|wyear)	11	18
colony_size + (1|site) + (1|wyear)	4	18
1 + (1|site) + (1|wyear)	3	20
ysd + (1|site) + (1|wyear)	4	22
1 + (1|site)	2	53

Table S6. Model summary for best-supported model indicating *Myotis velifer* count is a better predictor of *Pseudogymnoascus destructans* prevalence in the Southwest than overall colony count. Model selection based on second set of AIC comparisons (Table S5).

Variable	**Estimate**	**Std. Error**	**z value**	**p value**
(Intercept)	-15.170609	4.85769539	-3.1230055	0.00179014
speciesANPA	-1.809463	0.60181445	-3.0066792	0.00264118
speciesCOTO	-1.7364296	0.82150643	-2.1137139	0.03453971
speciesEPFU	1.11658103	1.40652784	0.79385633	0.42727908
speciesLANO	-18.070532	120152.192	-1.50E-04	0.99988
speciesMYCI	-0.945465	1.18799339	-0.7958504	0.42611899
speciesMYEV	-16.468766	10284.1916	-0.0016014	0.99872229
speciesMYTH	-1.3152744	0.90916211	-1.4466885	0.14798419
speciesMYVO	2.28482338	1.83089514	1.24792694	0.21205781
myveCount>1000	6.37045083	1.75549375	3.62886557	2.85E-04
r1_ysd_altered	15.061139	5.84118751	2.57843785	0.00992482